fishes

MDPI

Article

Transcriptome-Based Analysis of the Liver Response Mechanism of Black Porgy (*Acanthopagrus schlegelii*) to Stocking Density

Tangjian Zhou [1,2], Chaofeng Jia [2], Qian Meng [2], Dafeng Xu [2], Zhiwei Zhang [2], Fei Zhu [2], Yonglei Zhao [1,2], Ruijian Sun [2], Yunxia Yang [3,*] and Shuyin Chen [1,2,*]

[1] College of Fisheries and Life Science, Shanghai Ocean University, Shanghai 201306, China; etb89825598@163.com (T.Z.); m17348358603@163.com (Y.Z.)
[2] Jiangsu Marine Fisheries Research Institute, Nantong 226007, China; chaofeng.124@163.com (C.J.); mq1992917@163.com (Q.M.); xudafengqq@163.com (D.X.); zhzhwei2005@126.com (Z.Z.); ebancool@126.com (F.Z.); polly0055@163.com (R.S.)
[3] Fisheries College, Zhejiang Ocean University, Zhoushan 316022, China
* Correspondence: yangyx@zjou.edu.cn (Y.Y.); 13862908366@163.com (S.C.)

Abstract: Long-term high stocking density often brings negative effects such as decreased body weight, decreased immunity, and increased mortality to cultured fish, while the effects of short-term stocking are relatively less studied. In this experiment, we characterized spatial and temporal gene expression in black porgy (*Acanthopagrus schlegelii*) liver by establishing two stocking density groups—high (H: 26.5 kg/m^3) and low (L: 2.95 kg/m^3)—and conducting transcriptome sequencing before collecting liver samples at two time points: 6 h (AL and AH) and 60 d (CL and CH) into the culture trial. There were 648 and 550 differentially expressed genes (DEGs) in the AL-vs-AH and CL-vs-CH groups, respectively. The DEGs in the AL-vs-AH group were significantly enriched in steroid biosynthesis, terpenoid backbone biosynthesis, the PPAR signaling pathway, proteasome, aminoacyl-tRNA biosynthesis, and ribosome biogenesis in eukaryotes. The DEGs in the CL-vs-CH group were more significantly enriched in lipid metabolism-related pathways, such as the PPAR signaling pathway, fatty acid metabolism, and cholesterol metabolism. In addition, immune-related pathways such as the phagosome and complement and coagulation cascades were also enriched in the CL-vs-CH group. The expression changes concerning the DEGs in each group were further analyzed. The DEGs related to steroid synthesis, protein synthesis, and the degradation pathways were down-regulated, but immune-related genes were generally up-regulated in the AH group. The DEGs related to lipid synthesis were significantly up-regulated in the CH group, but the DEGs related to lipid consumption and utilization were down-regulated. The expression of immune-related DEGs was also negatively affected in the CH group. These results suggest that acute and chronic crowding stress affects lipid metabolism and immune regulation in the liver of black porgy. Acute stress particularly affected hepatic protein metabolism, while chronic stress showed more effects on hepatic lipid metabolism. The results of this study provide a theoretical basis for understanding the effects of high stocking densities upon black porgy and may also provide a reference for crowding stress regulation studies in other fish species.

Keywords: *Acanthopagrus schlegelii*; transcriptome; stocking density; acute stress; chronic stress

Key Contribution: The liver of black porgy has different molecular responses to short- and long-term high stocking density stress. Short-term high stocking density stress inhibited the transcription of genes related to peptide synthesis and degradation. Long-term high stocking density stress increased the transcription of genes related to lipid synthesis and inhibited the transcription of genes related to lipid utilization.

Citation: Zhou, T.; Jia, C.; Meng, Q.; Xu, D.; Zhang, Z.; Zhu, F.; Zhao, Y.; Sun, R.; Yang, Y.; Chen, S. Transcriptome-Based Analysis of the Liver Response Mechanism of Black Porgy (*Acanthopagrus schlegelii*) to Stocking Density. *Fishes* **2023**, *8*, 356. https://doi.org/10.3390/fishes8070356

Academic Editor: Eric Hallerman

Received: 12 June 2023
Revised: 6 July 2023
Accepted: 7 July 2023
Published: 8 July 2023

1. Introduction

With economic development and living standards increasing, the consumption of fisheries products is also increasing year by year. However, natural fishery resources cannot meet this increasing global demand. According to the 2022 edition of the State of World Fisheries and Aquaculture [1], sustainably harvested marine stock resources decreased by 1.2% in 2019 compared to 2017. Overfishing has seriously damaged fish stocks and ecosystems. To fulfill consumer demand and protect fishery resources and environments, increasing the proportion of cultured aquatic products is crucial for achieving sustainable industrial development. Fish is the main object of consumption in the aquatic market and has the largest portion of aquaculture [1]. In order to promote the stable and rapid development of cultured fish production, perfecting farming conditions and increasing stocking density could be crucial. Particularly, high-density, intensive aquaculture is viewed as an inevitable choice for the future of the aquaculture industry due to its ability to maximize the efficiency of culture systems. However, we must not overlook the adverse effects of excessively high stocking densities with respect to fish. High stocking densities could increase disease outbreak [2] and competition among individuals [3], leading to high mortality and significantly lower body weight [4,5]. In addition, stocking densities can change the fatty acids, amino acids, crude protein, and crude fat of fish muscle, affecting the nutritional value of the cultured fish products [4,6]. Therefore, improving the tolerance of fish to high stocking density culture and finding the optimal stocking density for fish culture are essential directions for aquaculture research.

Black porgy (*Acanthopagrus schlegelii*) is a benthic fish living in brackish and marine waters that is widely distributed in the coastal waters of the Western Pacific of the northern hemisphere [7]. With delicious meat and high nutritional value, black porgy is popular among consumers and valuable in the market. In China, Japan, and Korea, it is an important fish for farming due to its high growth rate and strong disease resistance [8,9]. Sea cage culture and pond culture are two mature ways of growing black porgy, but the limited yields make it difficult to scale up [10]. Moreover, apart from meeting market demand, some artificially propagated black porgies are used to restore the wild population in coastal areas [11]. Therefore, increasing the stocking density of black porgy can address consumption pressures and expedite the restoration of natural populations. However, there are few studies on the effect of high stocking densities on black porgy. The lack of relevant research is detrimental to black porgy welfare and production.

Transcriptome sequencing (RNA-seq) analysis can be powerful for understanding the crowding stress response caused by high stocking densities and determining the optimal fish culture density [12]. Upon the onset of stress, the sensing cells first generate signals due to external stimuli, which are later transmitted to target cells and cause physiological and biochemical responses within the target cells [13]. Ultimately, stress affects gene functions by inhibiting or promoting the transcriptional expression of genes within the cell, enabling the organism to respond to changes in the external environment to adapt to them. The transcriptional levels of cells can be altered within minutes of the onset of stress and can return to their basal transcriptional state upon the removal of stress [14]. Transcriptome sequencing can detect the mRNA transcript levels of all genes in a given tissue at a given time, helping to identify the genes affected by stress. Through the enrichment analysis of gene functions and pathways, the process of molecular changes in the organism in response to stress and the functional changes that may eventually develop can be determined [12]. Currently, transcriptome sequencing studies have been carried out for evaluating the effect of stocking density on many fish species, such as Nile tilapia (*Oreochromis niloticus*) [15], yellow croaker (*Larimichthys crocea*) [16], grass carp (*Ctenopharyngodon idellus*) [4,17], and rainbow trout (*Oncorhynchus mykiss*) [18]. These studies have revealed that gene regulation affects growth, metabolism, and immunity under high stocking densities, which laid the scientific and theoretical foundation for developing the production of these cultured species.

In this study, we describe how we performed short-term and long-term culture experiments on black porgy at different densities and collected livers under different treatment

conditions. We aimed to obtain the liver gene expression response to acute and chronic crowding stress to provide a basis for subsequent research and scientific guidance on the high-stocking density culture of black porgy.

2. Materials and Methods

2.1. Ethics Statement

All the experimental procedures described in this paper follow the international standards on animal welfare and were approved by the Institutional Review Board of Jiangsu Marine Fishery Research Institute (protocol code No. IRB 2017-02, 16 April 2017).

2.2. Experimental Animals

Black porgy juveniles (average body weight 88.49 ± 18.22 g and average body length 14.76 ± 1.12 cm [mean ± standard deviation]) were provided by the Jiangsu Province Black Porgy Breeding Farm located in Nantong. Before the start of the experiment, juvenile black porgies were temporarily held in an indoor concrete pond with a volume of 12.4 m^3 (3.08 m× 3.09 m × 1.30 m) for seven days, during which the water exchange rate was 50% per day.

2.3. Experimental Design and Sample Collection

The experiment began on 21 July and ended on 20 September. During the experiment, the fish were fed a compounded feed (crude protein ≥ 42%, crude fat ≥ 5%, crude fiber ≤ 5%, crude ash ≤ 16%, total phosphorus ≥ 1%, lysine ≥ 2.1%, and moisture ≤ 11%) with feeding to satiation at 07:30 and 17:00 daily. The residual feed was removed after 2 h. At the same time, the amount consumed and the number of pellets remaining were recorded. After sedimentation and filtration, natural seawater was used during the culture trial, with a 100% water change every two days. The temperature difference between water changes did not exceed 2 °C. To ensure uniform water quality in each group, the trial was conducted in a cement pond inside a plastic insulation shed housing six net pens measuring 1 m in length, 0.5 m in width, and 0.6 m in depth. Each net pen was equipped with at least one aeration stone. The key water quality parameters were as follows: temperature: 25.0~35.0 °C, pH: 7.30~8.50, and dissolved oxygen: ≥ 5 mg/L for 24 h during the trial.

Two treatment groups were established based on stocking density: low stocking density (L, 2.95 kg/m^3) and high stocking density (H, 26.5 kg/m^3), with three parallel groups created for each density level. To achieve better water quality consistency among different stocking density cages, net cages of groups L and H were alternately placed in the same cement pond. Group L was set based on the experience of black porgy culture in Nantong Lusi as the minimum stocking density with economic efficiency. Group H was established based on the recommendation of local farmers and the crowding stress densities of Sparidae such as gilthead seabream (*Sparus aurata*) [19] and red seabream (*Pagrus pagrus*) [20]. A total of 12 black porgies from groups L and H were randomly collected using plastic mesh boxes at two time points—the 6th hour and 60th day of the culture trial; 3 individuals in AL (short-term low stocking density), CL (long-term low stocking density), AH (short-term high stocking density), and CH (long-term high stocking density) group, respectively. AH and CH represents fish affected by acute and chronic crowding stress. The fish were not fed for at least 24 h before sample collection. During sampling, MS-222 was dripped into the plastic mesh box for rapid anesthesia, and the fish were then transported to the laboratory for dissection. An appropriate volume of liver tissue from each group was promptly frozen in liquid nitrogen and then preserved at −80 °C for further analysis. After the first sampling, the nets were supplemented with the same number of juvenile fish to maintain the experimental stocking density in each net.

2.4. Total RNA Extraction, cDNA Library Construction, and Sequencing

Three liver samples from three fish in each of the AL, AH, CL, and CH groups were retrieved after being frozen at −80 °C (with each individual serving as a biological replicate, three replicates per group). Each sample was individually homogenized, and total RNA was extracted using the Trizol kit (Invitrogen, Carlsbad, CA, USA), resulting in 12 total RNA samples. RNA integrity was evaluated via agarose gel electrophoresis with a 2:1 ratio of 28S:18S rRNA being utilized as the selected indicator. The OD (A260/280) of the nucleic acids was measured using a Nanodrop microspectrophotometer. The mRNA was enriched using oligo (dT) beads and then fragmented using a fragmentation buffer. The short fragments of mRNA were reverse-transcribed using the NEB #7530 kit (New England Biolabs, Inc., Ipswich, MA, USA). The purified double-stranded cDNA fragments were end-repaired, supplemented with A bases, and ligated using the Illumina sequencing adapter. The ligation reaction was purified with AMPure XP beads (1.0×), and polymerase chain reaction (PCR) amplification was performed. Both the beads and PCR primers were from the NEB #7530 kit. Sample fragment size and concentration were measured using the DNA 1000 assay Kit (Agilent Technologies, Santa Clara, CA, USA, 5067-1504). After obtaining a reliable cDNA library, Illumina Novaseq 6000 (Illumina, Inc., San Diego, CA, USA) sequencing was performed.

2.5. Sequencing Data Processing and Analysis

The raw reads were filtered using Fastp [21] for quality control (QC) to obtain clean reads. To guarantee the accuracy of the subsequent analysis, the base composition and quality distribution of the filtered data were examined. In case of mismatch rejection, reads matching with the *A. schlegelii* ribosome database were removed from the clean reads using the bowtie2 tool [22]. The remaining reads were mapped to the whole genome sequence of *A. schlegelii* using HISAT2 [9,23]. Stringtie [24] was used to reconstruct transcripts, and RNA-Seq by Expectation-Maximization (RSEM) [25] was used to quantify gene expression in each sample. Fragments per Kilobase Million (FPKM) was utilized as a metric to assess transcript abundance. After obtaining the expression results of each sample, principal component analysis (PCA) was carried out by the R package gmodels 2.18.1 to assess the repeat correlation between samples. The read count of gene expression data was also recorded into DESeq2 [26] for the analysis of differentially expressed genes (DEGs) using $|\log_2(\text{FoldChange})| > 1$ and FDR < 0.05 as screening criteria [4]. The DEGs were systematically analyzed with Gene Ontology (GO) and the Kyoto Encyclopedia of Genes and Genomes database (KEGG) to provide a comprehensive functional annotation and pathway analysis of the transcriptomics data [27–29]. Utilizing the hypergeometric test, we compared the DEGs mapped onto terms and pathways against the background gene set, thereby identifying significantly enriched GO terms and KEGG pathways.

2.6. RT-qPCR Verification

Eight DEGs in the AL-vs-AH and CL-vs-CH groups were selected for qPCR validation: thrombospondin 1 (*thbs1*), MHC Class-I Related-Gene Protein (*mr1*), fatty acid binding protein 1 (*fabp1*), fatty acid desaturase 2 (*fads2*), Acetyl-CoA carboxylase alpha (*acaca*), farnesyl pyrophosphate synthase (*fps*), sterol14α-demethylase (*cyp51*), and ATP-citrate lyase (*acly*).

The total RNA from each stocking density obtained during transcriptome sequencing and RT-qPCR were used to test the accuracy of the results derived from our transcriptome analysis. The FastQuant RT kit (Tiangen, Beijing, China) was used to synthesize cDNA templates according to the manufacturer's instructions. Nine DEGs (including the reference gene: β-actin) were selected based on the black porgy genome and transcriptome data. qPCR primers were designed using Oligo 7 software (https://www.oligo.net/demo-info2.html, accessed on 12 May 2023) (Table 1). qPCR quantification was performed using the SuperReal PreMix Plus kit (Tiangen, Beijing, China) and the Applied Biosystems 7300Plus Real-Time PCR System (Blk33, Singapore). The total volume of the PCR reactions was

20 µL (10 µL SYBR Green SuperReal PreMix Plus (2×), 0.6 µL each of forward and reverse primers, 2 µL cDNA, and 5.8 µL RNase-Free ddH_2O). Gene expression was quantified in batches of different primers at different annealing temperatures according to Oligo 7's recommendations. Other cycling conditions were set according to the kit's instructions. The qPCR quantification results were analyzed using the $2^{-\Delta\Delta Ct}$ method [30].

Table 1. Sequence of primers used for RT-qPCR expression analysis.

Gene Name	Primer Sequence (5′→3′)	Annealing Temperature/°C
thbs1	F: ATCCTGGCATTGCTGTTGGTTAC R: CGTCTCTGTCCGTGTTGATGAAG	56
mr1	F: GAACGAGGACATCATCACCAGAC R: ATCCAGCAGCACCGATAAGAATAAG	56
cela2a	F: TGTTACACTGATGGAGCCTGGAG R: GGTGAAGACGGTGGGTTTGTTC	56
fabp1	F: CCTGGAGACGATCACTGGAGAG R: GCCACCGACAGTCATAGTATTGC	56
fads2	F: GCCACCTGTCTGTCTTCAAGAAG R: AATGCCGATGATTCCACCAGTTG	55
acaca	F: TCAACAAGAAGTCAGAGCGAGAAG R: CACGGATGCCACTGCGATAC	54
fps	F: TGGAGGCAAGCGGAACAGAG R: ACCAGCCGACCAACAGAGC	58
cyp51	F: TCGGGAGCACATTCACCTACC R: CTGGAGTGGTTAGCCTGGAGTAG	58
acly	F: GTGATGGGAGAAGTTGGCAAGAC R: AGGAGGAAGTTGGCAGTGTGAG	59
β-actin	F: CGACGGTCAGGTCATCAC R: GCCAGCAGACTCCATTCC	56

3. Results

3.1. Transcriptome Sequencing Data Quality Analysis

In total, there were 85.82 Gb of raw data obtained through the transcriptome sequencing. The reads containing adapter sequences, more than 10% N, all A bases, or with more than 50% of bases having a quality (Q) $\leq$ 20 were removed. Finally, 84.29 Gb of clean data with 50.88~51.46% GC content, 97.64~98.42% Q20, and 92.71~95.21% Q30 were obtained (Table 2). The alignment results showed an average total mapping rate of 85.47%, with 76.83% of the reads mapped to reference genome sites with unique positions. Based on the total mapped reads results, 65.05~70.87% of the reads were located in exons in the reference genome (Table 3). These results show that the sequences have a highly reliable match with the reference genome of black porgy, verifying the reliability of the sequencing data.

Table 2. The statistics of assembled results for liver samples of *A. schlegelii*.

Sample	Raw_Data (bp)	Clean_Data (bp)	Q20	Q30	GC
AL-1	6,265,646,400	6,151,585,554	98.42%	95.21%	51.46%
AL-2	7,541,598,300	7,388,812,971	98.07%	93.91%	51.33%
AL-3	7,264,445,700	7,157,111,386	98.00%	93.92%	51.16%
AH-1	8,141,713,200	7,991,147,520	97.65%	92.71%	50.46%
AH-2	6,561,749,100	6,474,655,672	98.48%	95.39%	50.47%
AH-3	8,086,893,900	7,960,620,927	97.57%	92.75%	50.88%
CL-1	7,398,075,900	7,255,941,269	97.94%	93.53%	50.69%
CL-2	7,779,589,800	7,611,675,168	98.15%	94.12%	50.30%
CL-3	6,654,809,100	6,544,452,925	98.39%	95.06%	50.17%
CH-1	6,395,992,200	6,273,751,676	98.39%	95.13%	50.75%
CH-2	6,636,990,600	6,532,623,483	98.52%	95.46%	51.12%
CH-3	7,088,955,300	6,964,895,805	98.37%	95.11%	50.27%

Table 3. Matching of effective sequences with reference genomes of *A. schlegelii*.

Sample	Clean_Data	Unique_Mapped	Total_Mapped	Exon
AL-1	41,495,774	77.65%	86.30%	70.87%
AL-2	49,892,258	76.97%	85.85%	70.61%
AL-3	48,103,404	76.92%	85.82%	70.39%
AH-1	53,924,360	75.97%	84.13%	69.83%
AH-2	43,494,574	76.77%	85.07%	69.89%
AH-3	53,560,720	76.43%	84.78%	70.76%
CL-1	48,972,544	76.51%	85.67%	66.96%
CL-2	51,557,256	77.00%	85.71%	65.92%
CL-3	44,080,604	77.69%	86.16%	65.35%
CH-1	42,312,210	75.96%	85.20%	66.26%
CH-2	43,936,880	76.07%	85.79%	67.07%
CH-3	46,941,622	76.11%	85.20%	65.05%

3.2. Analysis of DEGs between Groups

Based on the gene expression information for each sample, the PCA results showed that the four groups—AL, AH, CL, and CH—were distinct, indicating that the gene expression patterns were different among the treatments under the design of this experiment (Figure 1). In this experiment, the DEGs in the AL-vs-AH group were defined as the up-or down-regulation of the DEG expression in the AH compared to the AL group, and so on for other comparisons. DEseq2 results showed that 648 DEGs were detected in the AL-vs-AH group (327 up-regulated and 321 down-regulated; Figure 2a). Meanwhile, a total of 550 DEGs were discovered in the CL-vs-CH group, with 213 DEGs being up-regulated and 337 DEGs down-regulated (Figure 2b). In comparing different culture density groups at the same time, 545 genes were found to be differentially expressed only in the AL-vs-AH group, while 447 genes were differentially expressed only in the CL-vs-CH group. A total of 103 genes showed differential expression in both comparison groups.

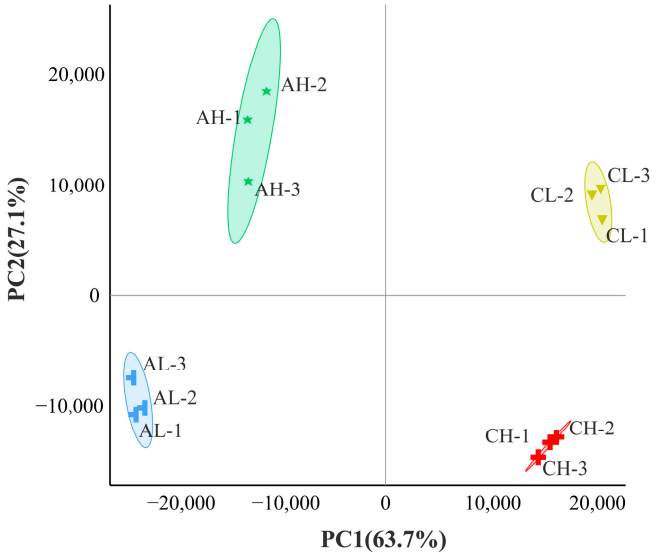

Figure 1. Principal component analysis (PCA) of gene expression in 12 samples. All 12 samples are labeled according to their groups, and samples classified as different clusters are shown with different-colored ellipses.

Further, comparing the same density treatment at different times, 1753 and 613 genes were exclusively differentially expressed in the AL-vs-CL and AH-vs-CH groups, respectively, with an additional 693 genes found to be differentially expressed in both groups. At the same sampling time for groups H and L, all factors except stocking density were kept the same, so the co-expressed DEGs revealed inherent stress response functions, while

the DEGs specific to each group reflected distinct adaptation patterns of response to acute and chronic stress (Figure 3). Both the H and L groups showed large differences in gene expression at different sampling times, which may be due to both the developmental growth of the fish and the temporal effect of different treatment intensities due to culture density, making it challenging to ensure that only a single stocking density factor exerted an influence. Based on these reasons, in the present study, we discuss and analyze the DEGs only between different stocking densities within the same sampling time to ensure the scientific reliability of the results.

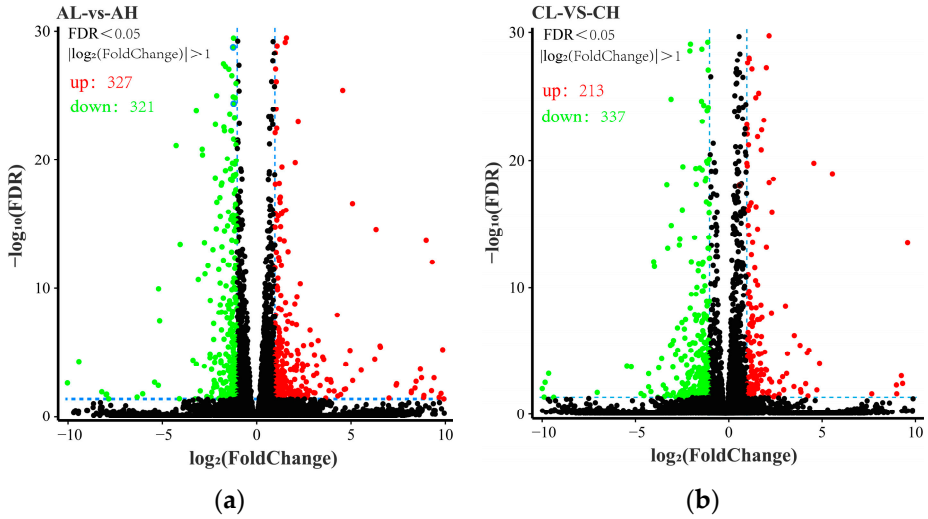

(**a**) (**b**)

Figure 2. Volcano plot of differentially expressed genes. (**a**) AL-vs-AH; (**b**) CL-vs-CH. The abscissa is the fold-change pertaining to gene expression in the high-density group compared with that in the low-density group, and the ordinate is the statistical significance of gene expression change. Different colors indicate up-regulated (red), down-regulated (green), and unchanged (black) gene levels regarding gene expression.

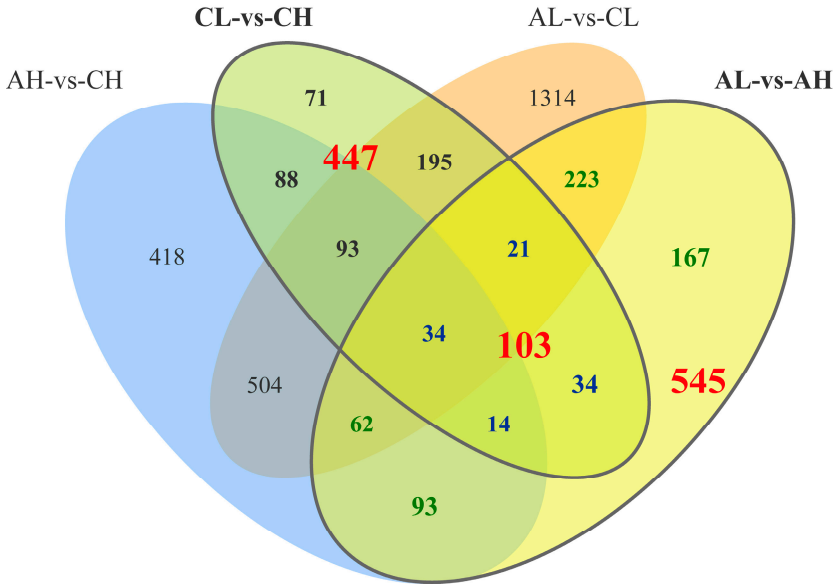

Figure 3. Venn diagram of DEGs for different comparisons among groups, indicated using different colors. Arabic numbers represent the number of differentially expressed genes. 447 represents the number of DEGs unique to the CL-vs-CH group compared to the AL-vs-AH group, 545 is the number of DEGs unique to the AL-vs-AH group compared to the CL-vs-CH group, and 103 is the number of DEGs shared by both groups.

3.3. GO Enrichment Analysis of DEGs

The DEGs among the AL-vs-AH and CL-vs-CH groups were processed for GO enrichment analysis to determine the molecular mechanisms involved in the crowding stress caused by different stocking densities of the liver of black porgy. Both the AL-vs-AH and CL-vs-CH DEGs were assessed according to the three main classifications of GO: biological process (BP), molecular function (MF), and cellular component (CC) (Figure 4). The AL-vs-AH and CL-vs-CH groups showed a total of 246 and 124 significantly enriched GO terms ($p < 0.05$), as well as 19 and 4 highly significantly enriched terms ($p_{adjust} < 0.05$), respectively.

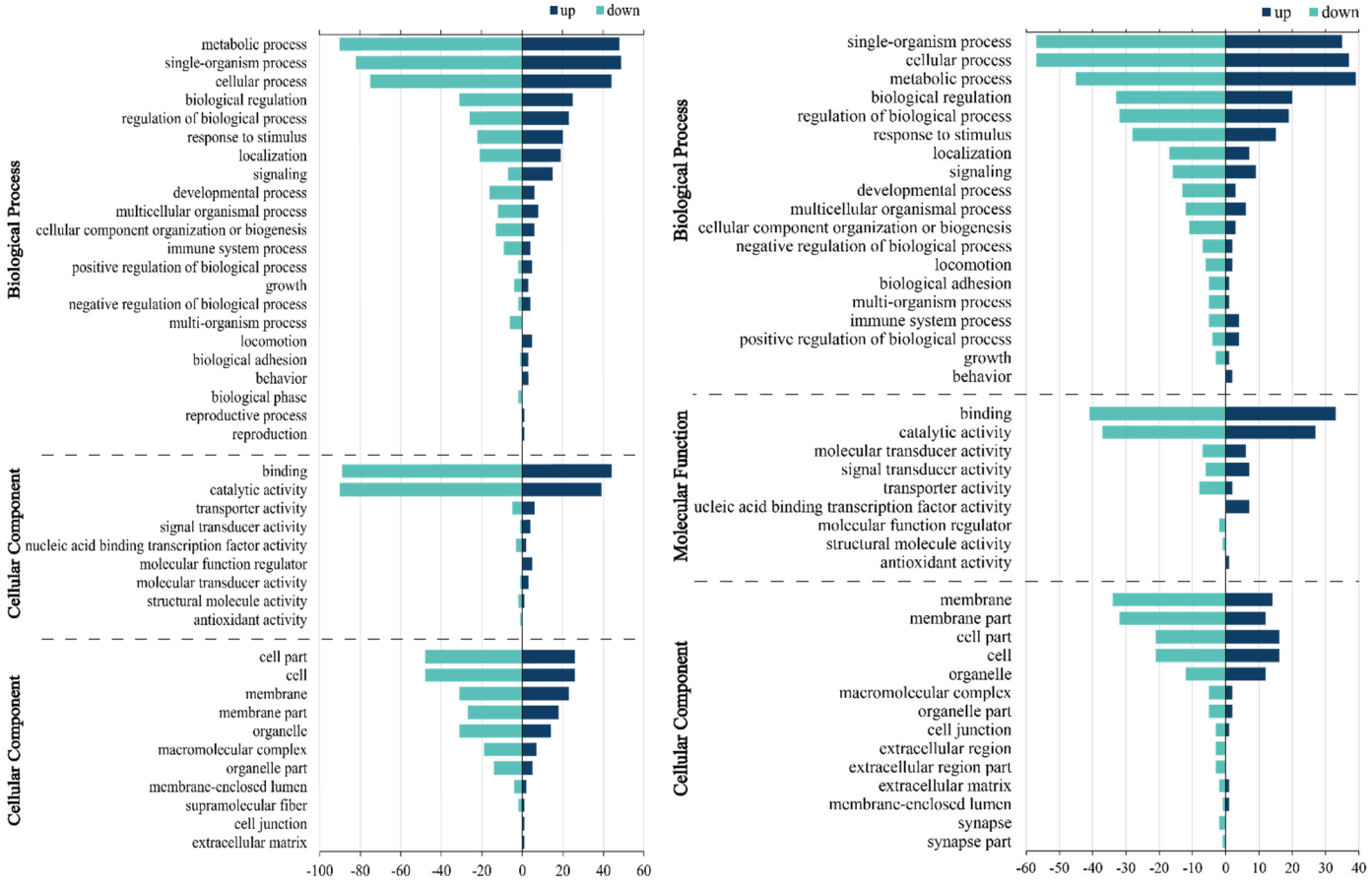

Figure 4. The classification of differentially expressed genes in three GO categories. (**a**) AL-vs-AH; (**b**) CL-vs-CH. The ordinate represents the other secondary GO items under the three major GO categories (i.e., BP, MF, and CC). The abscissa represents the number of DEGs included in each secondary classification, and the columns with different colors represent the number of up-regulated and down-regulated genes, respectively.

In AL-vs-AH, thirteen terms were highly significantly enriched in BP, including "tRNA aminoacylation for protein translation" and "single-organism metabolic process", which are related to peptide synthesis and metabolism, and "antigen processing and presentation of peptide antigen" and "defense response", which are related to the immune response. The DEGs enriched in "tRNA aminoacylation for protein translation" were down-regulated in the AL-vs-AH group. Six terms were highly significantly enriched in MF, mainly "aminoacyl-tRNA ligase activity" and "carboxylic ester hydrolase activity", which are related to catalytic activity, and the DEGs in these terms were down-regulated in the AL-vs-AH group.

In the CL-vs-CH group, there were four highly significantly enriched terms (all related to sulfotransferase activity involving sulfur-containing groups) sorted into the

molecular function (MF) category. These terms include "alcohol sulfotransferase activity", "phenanthrol sulfotransferase activity", "heparan sulfate sulfotransferase activity", and "sulfotransferase activity". All four terms were enriched for the same DEGs, which were down-regulated in the CL-vs-CH group. BP was mainly enriched in stress, metabolism, and immunity-related pathways such as "catechol-containing compound metabolic process", "steroid metabolic process", "chemokine production", "stress-activated MAPK cascade", "positive regulation of Toll-like receptor signaling pathway", and "response to other organism". Among them, the DEGs enriched in "response to other organism", "catechol-containing compound metabolic process", and "steroid metabolism" were down-regulated, while the DEGs enriched in "positive regulation of Toll-like receptor signaling pathway" and "chemokine production" were up-regulated in the CL-vs-CH group. The cellular component was mainly annotated for the "intrinsic component of membrane".

3.4. KEGG Enrichment Analysis of DEGs

Following our KEGG analysis, we found that 271 pathways were enriched in the AL-vs-AH group, among which 33 pathways showed significant enrichment ($p < 0.05$). Similarly, 253 pathways were enriched in the CL-vs-CH group, with 38 pathways showing significant enrichment. Some important pathways were selected for presentation from the top 30 pathways with the smallest p values in each group (Figure 5).

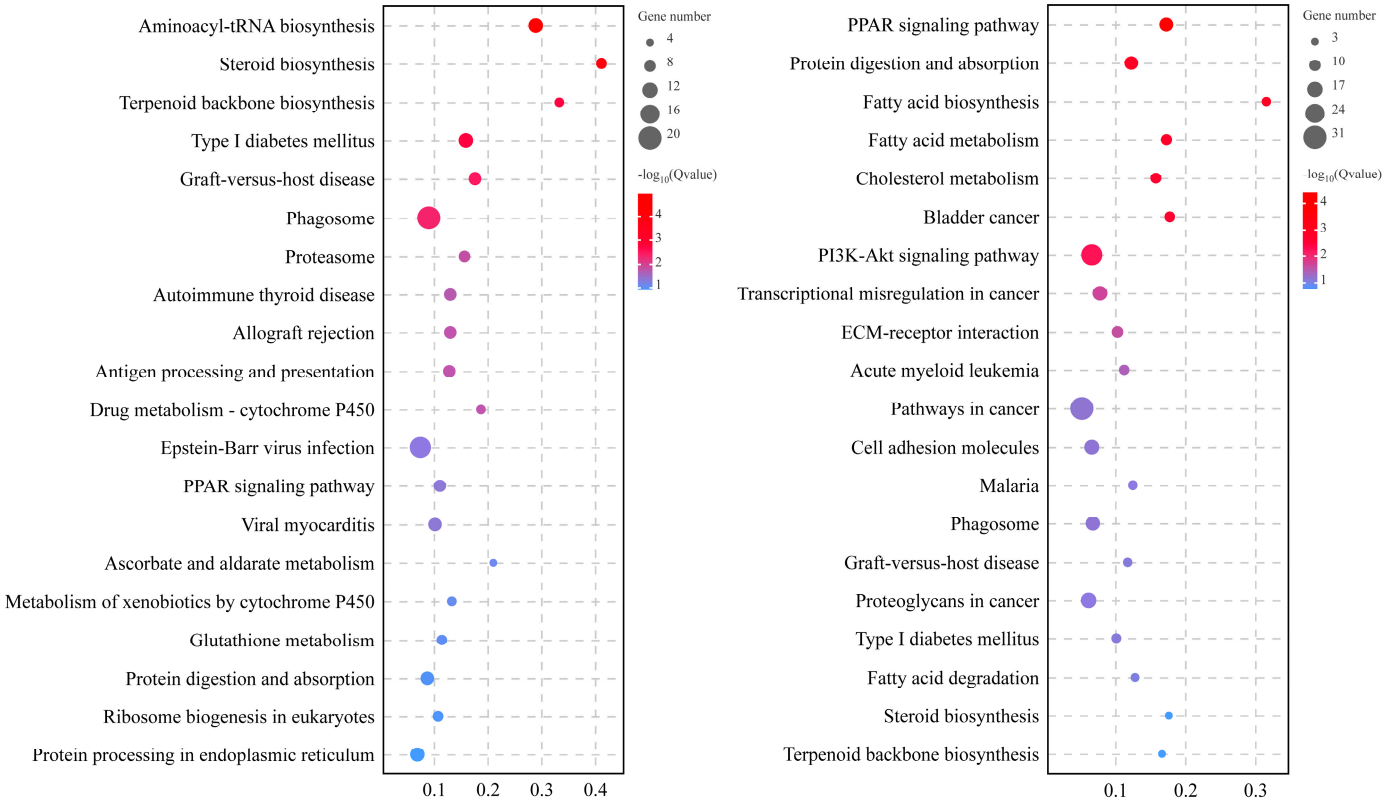

Figure 5. KEGG classification of DEGs. (**a**) AL-vs-AH; (**b**) CL-vs-CH. The abscissa is the gene ratio, the ordinate is the enrichment pathway, the sphere size represents the number of genes in this pathway, and the sphere color represents the enrichment significance of this pathway. Note: gene ratio refers to the proportion of DEGs detected in a pathway (relative to the total number of genes detected in that pathway).

According to the results of our KEGG enrichment analysis, significantly enriched pathways in the AL-vs-AH group included "aminoacyl-tRNA biosynthesis", "steroid biosynthesis", "terpenoid backbone biosynthesis", "phagosome", "proteasome", "antigen

processing and presentation", "protein digestion and absorption", etc. In the CL-vs-CH group, significantly enriched pathways mainly included immune and metabolic-related pathways such as the "PPAR signaling pathway", "protein digestion and absorption", "fatty acid biosynthesis", "fatty acid metabolism", "cholesterol metabolism", "PI3K-Akt signaling pathway", "ECM-receptor interaction", "phagosome", "AMPK signaling pathway", "complement and coagulation cascades", among others.

Based on the enrichment analysis results from GO and KEGG, we performed Gene-Set Enrichment Analysis (GSEA) to analyze the protein-related pathways in the AL-vs-AH group (Figure 6). The results showed that these pathways were significantly suppressed in the AL-vs-AH group.

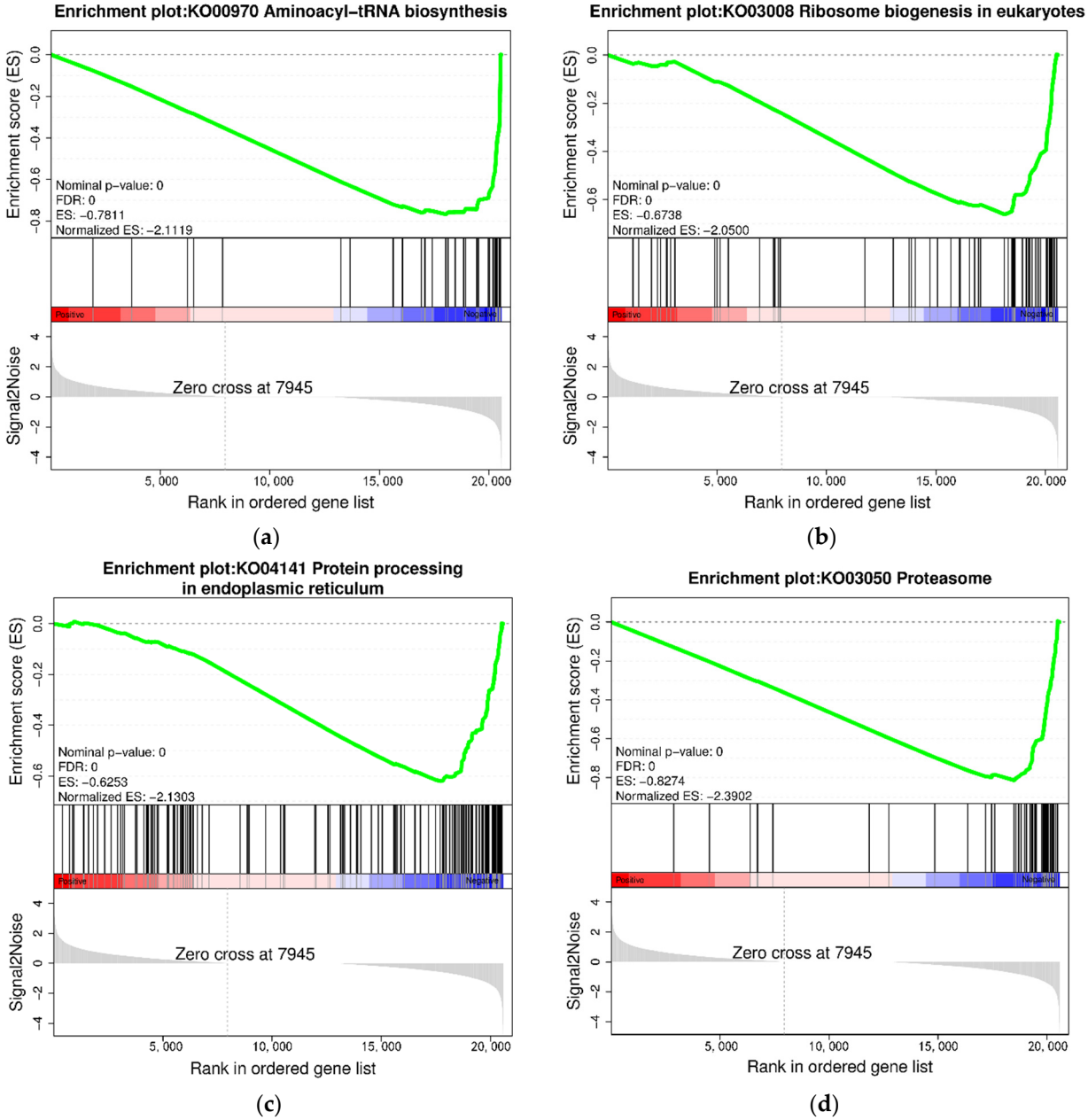

Figure 6. GSEA analysis of protein-related pathways in AL-vs-AH. The results showed that (**a**) aminoacyl-tRNA biosynthesis, (**b**) ribosome biogenesis in eukaryotes, (**c**) protein processing in endoplasmic reticulum, and (**d**) proteasome were significantly enriched and down-regulated.

3.5. Validation of RNA-Seq Results

The results in Figure 7 show that the expression trends of these genes in RT-qPCR were identical to the transcriptome results and had a high correlation. These results demonstrate the reliability and accuracy of the transcriptome sequencing and data analysis results.

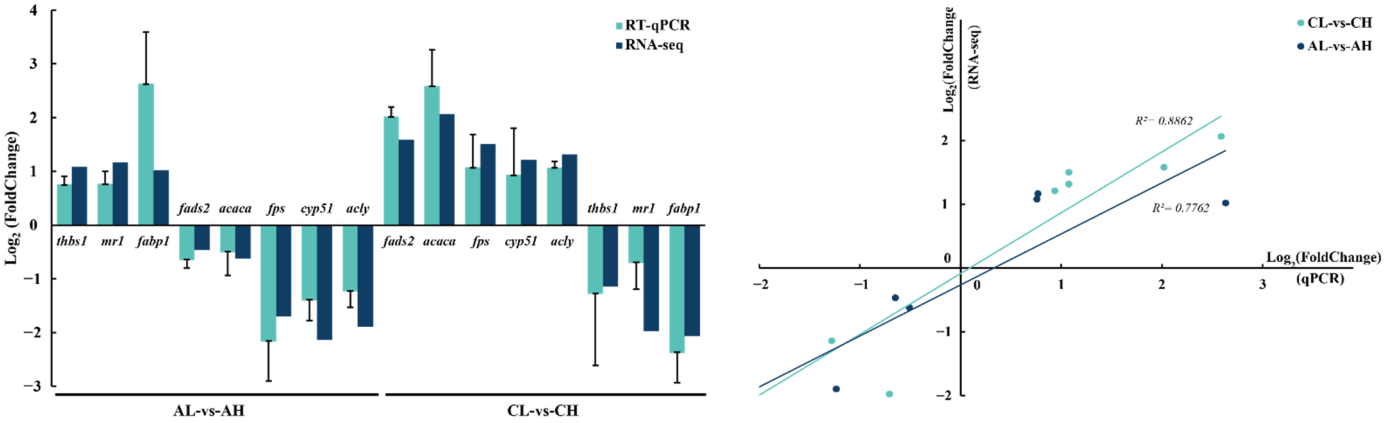

(**a**) (**b**)

Figure 7. RT-qPCR validation of 8 DEGs from AL-vs-AH and CL-vs-CH. The expression levels of the selected genes were each normalized to that of the β-actin. (**a**) Bar graph of expression trends in RNA-seq and qPCR. (**b**) Scatter plot of the correlation between RNA-seq and qPCR results.

4. Discussion

Studies on black porgy stress response have focused on aspects such as temperature [31], salinity [32], hypoxia [33], acidification [34], and feeding [35]. Previous studies have provided a scientific basis for achieving the optimal environmental conditions for black porgy culture. Inevitably, the aquaculture industry is moving towards industrial, high-density production. However, stress arising from overcrowding significantly impacts fish growth, immunity, and metabolism [36]. As an important farmed fish, few studies have reported the effect of stocking density on black porgy.

The liver, a reliable tissue for transcriptome research, is the largest digestive gland in fish, the primary response organ to stress, and the central metabolic organ with roles in detoxification, immune defense, and hormone synthesis in the organism [37–39]. In this experiment, we observed significantly different gene expression profiles, indicating the effects of different stocking densities and culture times on black porgy. A total of 1198 DEGs were obtained after subjecting the samples to transcriptome analysis, and several biological pathways potentially related to crowding stress, along with their key genes were identified.

4.1. Effects of High Stocking Density on Protein Metabolism-Related Pathways

Protein is an essential material basis for the realization of life functions. Aquatic animals facing acute environmental stresses such as heat stress [40], hypoxia [41], and hyposalinity [42] generally experience the inhibition of protein synthesis. This phenomenon has primarily been attributed to alterations in enzyme activity, disruptions in cellular ion homeostasis, or an increased need for energy in response to environmental stressors. High stocking density as a stressor may also lead to changes in functions associated with protein synthesis [43]. In this experiment, after being subjected to 6 h of crowding stress, the liver of black porgy was mainly enriched in the expression of some significant pathways related to protein metabolism, such as aminoacyl-tRNA biosynthesis, ribosome biogenesis in eukaryotes, protein processing in endoplasmic reticulum, and proteasome. The aminoacyl-tRNA biosynthesis pathway, activated by amido-tRNA synthetase, plays a crucial role in converting amino acids into proteins by precisely connecting them to tRNAs containing the corresponding anticodons, thereby ensuring accurate protein synthesis [44]. Ribosome

biogenesis in eukaryotes includes the maturation of ribosomal RNA and assembly into ribosomal subunits [45]. Ribosome biogenesis determines the rate of protein synthesis and regulates the accumulation of cell mass or cell growth by controlling the major anabolic cellular processes [46]. The endoplasmic reticulum is involved in protein synthesis, folding, and processing and directs misfolded proteins to the proteasome for degradation [47]. The ubiquitin-proteasome system (UPS) mediates 80~90% of protein degradation in eukaryotic organisms [48]. Ubiquitination is a post-translational energy-dependent modification process that labels soon-to-be-degraded proteins and involves activation (ubiquitin activation enzyme E1), conjugation (ubiquitin conjugase E2), and ligation (ubiquitin ligase E3) [49]. Ubiquitin-like modifier-activating enzyme 1 (UBA1) and ubiquitin-like modifier-activating enzyme 6 (UBA6) are the two types of E1 enzymes responsible for activating ubiquitin [50]. Upon examining the results of our GSEA analysis, we found that, among the expression of pathways and genes related to protein synthesis, *uba1* and *uba6* were associated with the activation of the ubiquitination process and that related genes in the proteasome were down-regulated, indicating that these pathways were inhibited in the AL-vs-AH group. These pathways may provide energy in response to stress by temporarily inhibiting the protein synthesis of normal cellular maintenance processes.

In contrast, the CL-vs-CH group did not exhibit significant enrichment, nor did the pathways observed in the AL-vs-AH group. This suggests that these pathways were responsive only during the early stages of crowding stress and eventually returned to baseline expression after adaptation to the environment in black porgy. These changes were also consistent with the functional characteristics of the related pathways that maintain the basic activities needed for daily functioning.

4.2. Effects of High Stocking Density on Lipid Metabolism-Related Pathways

Lipids are important energy substances for fish, helping them to respond to acute stresses [51,52]. The PPAR signaling pathway, steroid biosynthesis, terpenoid backbone biosynthesis, and other lipid metabolism pathways were significantly enriched after 6 h of crowding stress. Fatty-acid transport protein 2 (*fatp2*), cholesterol 7α-hydroxylase (*cyp7a1*), and *fabp1* are critical genes in the PPAR signaling pathway. The FATP family is involved in the uptake and metabolism of long-chain and extra-long-chain fatty acids and plays a key role in the coordinated utilization of energy [53]. FABP1 is active in lipid metabolism in various tissues and organs, involved in lipid uptake and transport, and has a role in maintaining lipid homeostasis [54]. Following acute crowding experiments on *O. mykiss*, Naderi et al. [43] found that the up-regulation of FABP was associated with an increase in lipid utilization, which occurred in order to meet increased energy requirements due to stress. CYP7A1 is a rate-limiting enzyme expressed only in the liver for the synthesis and conversion of cholesterol into bile acids [38]. Bile acids contribute to energy conservation, improve energy utilization efficiency, and play a pivotal role in maintaining the balance of cholesterol metabolism [55]. In the AL-vs-AH group, the up-regulation of *fabp1* and *fatp2* may indicate that black porgy supplied the energy required for stress response by increasing lipid utilization under acute crowding stress, and the up-regulation of *cyp7a1* may benefit the energy stabilization of black porgy under acute crowding stress conditions. Steroid biosynthesis is associated with the mevalonate pathway in the equally enriched terpenoid backbone biosynthesis. The primary function of the mevalonate pathway is to synthesize cholesterol and isoprenoids [56]. 3-Hydroxy-3-methylglutaryl-coenzyme A synthase 1 (HMGCS1) and 3-hydroxy-3-methylglutaryl-coenzyme A reductase (HMGCR) are two key rate-limiting enzymes associated with the mevalonate pathway and the cholesterol synthesis pathway [57]. HMGCS1 catalyzes HMG-CoA synthesis from acetoacetyl-CoA and acetyl-CoA, which HMGCR subsequently reduces to mevalonate acid (MVA). Farnesyl pyrophosphate (FPP), generated by MVA after a series of catalytic processes, is a precursor for steroid synthesis [56]. The steroid biosynthesis pathway produces mainly steroid hormone precursors, cholesterol, and vitamin intermediaries [58]. Squalene epoxidase (*sqle*), sterol-c5-desaturases (*sc5d*), carboxyl ester lipase (*cel*), transmembrane 7 superfamily

member 2 (*tm7sf2*), methylsterol monooxygenase 1 (*msmo1*), and *cyp51* are all DEGs in the steroid biosynthesis pathway of AL-vs-AH. SQLE is involved in the first oxygenation step of the cholesterol biosynthesis pathway [59]. Inhibiting *sqle* expression can significantly reduce steroid production [60]. *sc5d*, *cel*, *tm7sf2*, *msmo1*, and *cyp51* are involved in the synthesis or conversion of cholesterol [61–63]. Fish respond to stress by inhibiting the steroid biosynthesis pathway when subjected to acute stresses such as hypoxia [64] and high temperatures [65]. This pathway is also closely related to energy balance under stress. Similarly, the expression levels of *hmgcr*, *hmgcs1*, *sc5d*, *cel*, *tm7sf2*, *msmo1,* and *cyp51* (genes related to steroid metabolism) were significantly down-regulated in AL-vs-AH, which may also indicate that lipid metabolism represented by steroids is involved in energy homeostasis under acute crowding stress. Notably, *hmgcr* was down-regulated in AL-vs-AH, and this contrasts with the up-regulated expression observed in European sea bass (*Dicentrarchus labrax*) [66] subjected to chronic crowding stress. This may result from differences in the response patterns of fish to different temporal stages of crowding stress.

Lipid metabolism seems more significantly affected under long-term high stocking densities. At the tissue level, the hepatosomatic index of *S. aurata* was significantly down-regulated and liver fatty acid composition was significantly altered [67]. At the molecular level, many pathways related to lipid metabolism were found to be enriched in different species of fishes [68,69]. After suffering chronic crowding stress, black porgy significantly enriched many pathways related to lipid metabolism, such as fatty acid biosynthesis, cholesterol metabolism, the AMPK signaling pathway, the PPAR signaling pathway, steroid biosynthesis, and terpenoid backbone biosynthesis. Acyl-CoA synthetase short-chain family member (*acss2*), fatty acid synthase (*fasn*), stearoyl-CoA desaturase-1 (*scd1*), carnitine palmitoyl transferase 1A (*cpt1a*), isopentenyl-diphosphate delta-isomerase 1 (*idi1)*, ATP binding cassette transporter A1 (*abca1*), fatty acid transport protein1 (*fatp1*), *acly*, *fps*, *acaca*, *fads2*, *fabp1*, and *cyp51* are DEGs belonging to the CL-vs-CH group that relate to lipid metabolism. ACLY and ACSS2 are the main sources of acetyl CoA in the nucleus and cytoplasm [70]. ACACA is involved in the first step of fatty acid synthesis and is also a key rate-limiting enzyme in this reaction, facilitating the catalytic conversion of acetyl CoA to malonyl CoA [71,72]. Subsequently, malonyl CoA undergoes successive condensation reactions with acetyl CoA in the presence of FASN, another key rate-limiting enzyme for fatty acid synthesis, to produce long-chain saturated fatty acids [46,71]. SCD1 and FADS2 exhibit fatty acid desaturation activity, wherein they can convert long-chain saturated fatty acids into their unsaturated counterparts. FADS2 is a key rate-limiting enzyme for biosynthesis in polyunsaturated fatty acids (PUFAs) [73]. At the same time, SCD1 specifically converts the long-chain saturated fatty acids into monounsaturated fatty acids (MUFA) and confers an inhibitory effect on the fatty acid β-oxidation mechanism [74]. CPT1A can promote mitochondrial β-oxidation by helping acyl-CoA (acyl-CoA) to enter the mitochondrial matrix and is a key rate-limiting enzyme for mitochondrial fatty acid β-oxidation [75]. In addition, mitochondria are also the main site of hepatic fatty acid β-oxidation in *S. aurata* [69] under chronic crowding stress. FPS could synthesize FPP, a cholesterol, steroid, and dolichol precursor [56]. IDI1 is a key enzyme in the mevalonate pathway and is important in promoting cholesterol synthesis [76]. ABCA1 controls cholesterol efflux from hepatocytes [77]. In the CL-vs-CH group, the increase in *acly*, *acss2*, *acaca*, and *fasn* expression could promote the production of acetyl CoA and the subsequent synthesis of saturated fatty acids. The up-regulation of *scd1* and *fads2* promoted the conversion of saturated fatty acids to unsaturated fatty acids. Similarly, the up-regulation of *fps*, *idi1*, and *cyp51* may promote hepatic steroid synthesis. Notably, in fish subjected to chronic crowding stress, cortisol (a steroid hormone) plays a pivotal role in immunosuppression [78,79]. The activation of steroid synthesis in the liver of black porgy during chronic stress may lead to elevated cortisol levels, ultimately resulting in immunosuppression in the organism. Conversely, *fatp1*, *fabp1*, *cpt1a*, and *abca1* were notably observed to be down-regulated. The PPAR signaling pathway promotes the β-oxidation of fatty acids and regulates fatty acid metabolism [80,81]. In a related study investigating chicks, a decrease in the expression of the *fabp* gene (sited upstream of the PPAR

signaling pathway) impeded the normal function of the PPAR signaling pathway, thus causing disturbances in lipid metabolism [82]. Inhibition of the PPAR signaling pathway in the liver was also found in long-term high-density culture trials with largemouth bass (*Micropterus salmoides*) [68] and tiger puffer (*Takifugu rubripes*) [83]. Hence, it is plausible to suggest that the PPAR signaling pathway may have been inhibited in the CH group in this experiment. Furthermore, its hepatic mitochondrial β-oxidation and cholesterol efflux was also inhibited. These factors may lead to hepatic lipid accumulation in black porgy. According to these results, it has become evident that chronically crowded black porgy had an upsurge in liver fatty acid synthesis, coupled with a decline in the efficiency of lipid utilization. These findings suggest a disruption in lipid metabolism, which could potentially impact various physiological aspects of the fish, including growth, feeding, immunity, and stress tolerance [84,85].

4.3. Effects of High Stocking Density on Immunity

Acute stress is often linked to a disturbance in homeostasis and tissue damage in the organism. In acute crowding conditions (where frictional contact between bodies is frequent), skin damage can occur, increasing susceptibility to waterborne pathogens [86]. Consequently, utilizing stress-induced immunoprotective mechanisms to bolster immune defense during injury, infection, and vaccination is a crucial strategy for animals to adapt to their ever-changing environments [87]. Most published data suggest that acute stress promotes the activity of innate immune response pathways in fish and triggers the up-regulation of pro-immune genes in both primary and non-primary immune organs [88,89]. In this experiment, several immune-related genes were enriched in the acute crowding stress group, such as NADPH oxidase 1 (*nox1*), interleukin-8 (*il-8*), C-C motif chemokine ligand 20 (*ccl20*), proteinase-activated receptor 2 (*f2rl1*), NADPH oxidase 2 (*nox2*), matrix metalloproteinase 9 (*mmp9*), glutathione-S-transferase alpha 4 (*gsta4*), glutathione peroxidase 8 (*gpx8*), forkhead box O1A (*foxo1a*), inositol oxygenase (*miox*), and thrombospondin 1 (*thbs1*). In the liver, NADPH oxidases (NOX1, NOX2, and NOX4) are recognized as the primary source of non-mitochondrial H_2O_2 [90]. More specifically, hepatocytes express NOX1, NOX2, and NOX4, while phagocytes and other immune cells primarily exhibit NOX2 expression [91]. MMP9, also called gelatinase B, is a key player in the innate immune responses of fish. It is primarily secreted by endothelial cells, leukocytes, fibroblasts, neutrophils, and macrophages in an inactive or proenzyme form [92]. Its critical role involves facilitating the migration of leukocytes to the site of inflammation by breaking down extracellular matrix components and releasing chemokines and cytokines [93]. The overexpression of *miox* could accelerate reactive oxygen species (ROS) production and NADPH depletion, enhance oxidative stress damage, and induce programmed cell death [94]. The expression of *gsta4* can be induced by ROS to protect cells against oxidative stress-induced damage [95]. Furthermore, GPX8 positively contributes to the scavenging of H_2O_2 produced from ROS [96]. Deficiencies in *foxo1a*, a vital gene involved in cellular oxidative stress and apoptosis, are associated with increased oxidative stress [97]. Acute stress usually affects the distribution of immune cells. Immune cells are transported to organs such as the skin and peripheral tissues during or after acute stress. This results in enhanced immune function in relevant tissues such as the skin, while immune function in tissues such as the blood and spleen, where immune cells are temporarily depleted during acute stress, is shown to be suppressed [87]. In *S. aurata*, acute crowding stress experiments have identified the transfer of phagocytes from the head kidney to the blood [98]. The down-regulation of *nox2* and *mmp9* in the AL-vs-AH group may indicate a possible similar phenomenon in the liver of black porgy under acute crowding stress. However, a notable increase in the up-regulation of pro-immune-related genes, including *nox1*, *thbs1*, *il-8*, *ccl20*, and *f2rl1*, was also observed, indicating the involvement of the liver in immune adaptation to dynamic environmental changes through the activation of associated genes. In addition, the expression of key genes of the antioxidant-related glutathione and ascorbic acid pathways, such as *gsta4*, *gpx8*, *foxo1a*, and *miox*, were up-regulated in AL-vs-AH. Oxidative stress refers to the excessive production of highly

reactive molecules such as ROS and reactive nitrogen species (RNS) free radicals in the body in response to various harmful stimuli, which exceeds the scavenging capacity of oxidants, resulting in a dynamic imbalance between the oxidative and antioxidant systems and leading to tissue damage [99]. It has also been shown that crowding stress can lead to oxidative stress and oxidative damage in fish [68,100]. Changes in the expression of *gsta4*, *gpx8*, *foxo1a*, and *miox* may represent a degree of oxidative stress in the liver under acute crowding stress. Black porgy avoided stress damage by up-regulating antioxidant genes.

Compared to enhancing immune capacity by acute stress, chronic stress negatively impacts immune ability in mammals and fishes [87,88,101]. Long-term high-density culture is a chronic stress for fish. Immunosuppression caused by crowding stress generated by high long-term stocking densities has been found in turbot (*Scophthalmus maximus*) [102,103], Atlantic salmon (*Salmo salar*) [104], *O. mykiss* [105], and *L. crocea* [16]. In essence, this suppression of innate and adaptive immune responsiveness is achieved through a neuroendocrine mechanism, the hypothalamic–pituitary–interrenal axis (HPI axis), to maintain energy conservation under chronic stress and reduce autoimmune damage [88]. Cortisol, one of the foremost stress hormones of the HPI axis, stands out as the primary hormone that mediates the immunosuppressive effects of chronic stress [101]. In the CL-vs-CH group, various immune-related pathways exhibited alterations, including complement and coagulation cascades and phagosome. There were also pathways related to immunity in other organisms, including malaria, the AGE/RAGE signaling pathway in diabetic complications, and leishmaniasis. Consistent with prior research, numerous immune genes discovered within these pathways—such as neutrophil cytosolic factor 4 (*ncf4*), integrin alpha-L (*itgal*), integrin alpha m (*itgam*), transforming growth factor beta 3 (*tgb3*), C-X-C motif chemokine receptor 2 (*cxcr2*), complement C1s (*c1s*), complement C1q C chain (*c1qc*), *thbs1*, *f2rl1*, and *il-8*—were identified as being down-regulated. THBS1 is involved in activating a variety of inflammatory cells and regulating cell adhesion and migration in inflammation [37]. In both the liver of tongue sole (*Cynoglossus semilaevis*) [37] and three-spined stickleback (*Gasterosteus aculeatus*) [106], *thbs1* plays a crucial role in immune regulation. IL-8 plays an essential role in the inflammatory response, and CXCR2 participates in various immune responses by specifically recognizing IL-8 to activate a series of signaling processes [107]. The complement system is involved in innate and adaptive immunity. It significantly contributes to inflammation, immune complex clearance, the induction of normal humoral immune responses, and the clearance of apoptotic cells [108]. The classical pathway is one of the activation pathways of the complement system. Its initiation relies on binding the Fc portion of the immune complex, formed by the binding of IgG or IgM to pathogens or non-self antigens, to the C1 complex [109]. The C1 complex is a multimeric complex composed of C1q, C1r, and C1s [110]. The inhibition of fish complement system function induced by chronic crowding stress has also been reported [67,111]. The results of the preset study indicate that the expression of important immune-related genes in the liver was suppressed after long-term high-density culture, which may reduce the defense ability of black porgy against diseases.

5. Conclusions

Our findings reveal the significant effects of short- and long-term high stocking densities on protein synthesis and degradation, lipid metabolism, and immune response. Correspondingly, these effects could be used as indicators of the crowding stress experienced by the fish in aquaculture. Depending on the duration of production, black porgy undergoes distinct physiological adaptation processes. In short-term high-stocking-density production, fish respond to acute crowding stress by altering their protein and steroid synthesis to meet the demands of energy homeostasis. The activation of immune- and antioxidant-related pathways meets the immune defense requirements of the organism under acute stress. Long-term high stocking density production, on the other hand, causes chronic crowding stress. Under this condition, black porgy may have more fatty acid production but less efficient lipid use and a decrease in immune factor expression. In

conclusion, our study reveals the molecular response mechanisms of black porgy liver under different conditions of overcrowding stress and emphasizes the importance of proper density management in ensuring the healthy and sustainable farming of black porgy. These results provide a foundation for further research on species- and tissue-specific molecular regulatory response mechanisms under crowding stress conditions.

Author Contributions: T.Z. and C.J. conceived and designed the study. T.Z., Q.M. and R.S. were responsible for the fish rearing and sampling. D.X. and F.Z. performed the RNA-seq and qPCR analyses. T.Z., Z.Z. and Y.Z. analyzed the data and wrote the manuscript. S.C. and Y.Y. made modifications to the article and provided guidance for the experiment. All authors have read and agreed to the published version of the manuscript.

Funding: This research was funded by the Creation of Agricultural Major New Varieties of Jiangsu Province (grant number: PZCZ 201744), the "JBGS" Project of Seed Industry Revitalization in Jiangsu Province (JBGS(2021)034), and the Youth Science and Technology Talent innovation Project of Nantong City (JC12022040).

Institutional Review Board Statement: The study was conducted in accordance with the Declaration of Helsinki and approved by the Institutional Review Board (or Ethics Committee) of the Jiangsu Marine Fishery Research Institute (protocol code No. IRB 2017-02, 16 April 2017, Nantong, China).

Data Availability Statement: The raw transcriptomic data generated in this study have been deposited in the NCBI's SRA (Sequence Read Archive) under the accession number PRJNA991263. The data can be accessed at the following URL: (https://dataview.ncbi.nlm.nih.gov/object/PRJNA991263?reviewer=gdc1cbtkncvbu7a92e8rk3v8jp, accessed on 6 July 2023).

Conflicts of Interest: The authors declare that there are no known competing financial interests or personal relationships that could have influenced the reporting of the work in this paper.

References

1. FAO. *The State of World Fisheries and Aquaculture 2022*; FAO: Rome, Italy, 2022; ISBN 978-92-5-136364-5.
2. Garcia, F.; Romera, D.M.; Gozi, K.S.; Onaka, E.M.; Fonseca, F.S.; Schalch, S.H.C.; Candeira, P.G.; Guerra, L.O.M.; Carmo, F.J.; Carneiro, D.J.; et al. Stocking Density of Nile Tilapia in Cages Placed in a Hydroelectric Reservoir. *Aquaculture* **2013**, *410–411*, 51–56. [CrossRef]
3. Mishal, P.; Karnatak, G.; Das, B.K.; Tayung, T.; Kumari, S.; Sarkar, U.K.; Das, A.K.; Ali, Y. Impact of Stocking Density on Growth, Feed Utilization and Survival of Cage Reared Minor Carp, *Labeo bata* (Hamilton, 1822) in Maithon Reservoir, India. *Aquaculture* **2021**, *532*, 736078. [CrossRef]
4. Zhao, H.H.; Soufan, O.; Xia, J.G.; Tang, R.; Li, L.; Li, D.P. Transcriptome and Physiological Analysis Reveal Alterations in Muscle Metabolisms and Immune Responses of Grass Carp (*Ctenopharyngodon idellus*) Cultured at Different Stocking Densities. *Aquaculture* **2019**, *503*, 186–197. [CrossRef]
5. Wang, Y.Y.; Ni, J.J.; Nie, Z.J.; Gao, J.C.; Sun, Y.; Shao, N.L.; Li, Q.J.; Hu, J.W.; Xu, P.; Xu, G.C. Effects of Stocking Density on Growth, Serum Parameters, Antioxidant Status, Liver and Intestine Histology and Gene Expression of Largemouth Bass (*Micropterus salmoides*) Farmed in the in-Pond Raceway System. *Aquac. Res.* **2020**, *51*, 5228–5240. [CrossRef]
6. Liu, Q.; Hou, Z.S.; Wen, H.S.; Li, J.F.; He, F.; Wang, J.H.; Guan, B.; Wang, Q.L. Effect of Stocking Density on Water Quality and (Growth, Body Composition and Plasma Cortisol Content) Performance of Pen-Reared Rainbow Trout (*Oncorhynchus mykiss*). *J. Ocean. Univ. China* **2016**, *15*, 667–675. [CrossRef]
7. Zhou, F.; Song, W.X.; Shao, Q.J.; Peng, X.; Xiao, J.X.; Hua, Y.; Owari, B.N.; Zhang, T.Z.; Ng, W.K. Partial Replacement of Fish Meal by Fermented Soybean Meal in Diets for Black Sea Bream, *Acanthopagrus schlegelii*, Juveniles. *J. World Aquac. Soc.* **2011**, *42*, 184–197. [CrossRef]
8. Jin, M.; Pan, T.T.; Cheng, X.; Zhu, T.T.; Sun, P.; Zhou, F.; Ding, X.Y.; Zhou, Q.C. Effects of Supplemental Dietary L-Carnitine and Bile Acids on Growth Performance, Antioxidant and Immune Ability, Histopathological Changes and Inflammatory Response in Juvenile Black Seabream (*Acanthopagrus schlegelii*) Fed High-Fat Diet. *Aquaculture* **2019**, *504*, 199–209. [CrossRef]
9. Zhang, Z.Y.; Zhang, K.; Chen, S.; Zhang, Z.W.; Zhang, J.Y.; You, X.X.; Bian, C.; Xu, J.; Jia, C.F.; Qiang, J.; et al. Draft Genome of the Protandrous Chinese Black Porgy, *Acanthopagrus Schlegelii*. *Gigascience* **2018**, *7*, giy012. [CrossRef]
10. Jia, C.F.; Zhu, F.; Qiu, M.; Sun, R.J.; Liu, H.L.; Zhang, Z.W.; Chen, S.Y.; Xu, J.; Zhang, Z.Y. Effects of low-salinity water cultivation on nutrient components of black porgy (*Acanthopagrus schlegelii*). *Sci. Technol. Food Ind.* **2020**, *41*, 284—288+294. [CrossRef]
11. Garcia Garcia, B.; Basurco, B.; Lovatelli, A. Current Status of Sparidae Aquaculture. In *Sparidae: Biology and Aquaculture of Gilthead Sea Bream and Other Species*; John Wiley & Sons, Inc.: Hoboken, NJ, USA, 2011; pp. 1–50, ISBN 978-1-4051-9772-4.
12. Qian, X.; Ba, Y.; Zhuang, Q.F.; Zhong, G.F. RNA-Seq Technology and Its Application in Fish Transcriptomics. *OMICS A J. Integr. Biol.* **2014**, *18*, 98–110. [CrossRef]

13. Macdonald, J. Signal Transduction Pathways and the Control of Cellular Responses to External Stimuli. In *Functional Metabolism: Regulation and Adaptation*, 1st ed.; Storey, B., Ed.; John Wiley & Sons, Inc.: Hoboken, NJ, USA, 2005; pp. 87–123, ISBN 978-0-471-67558-7.
14. De Nadal, E.; Ammerer, G.; Posas, F. Controlling Gene Expression in Response to Stress. *Nat. Rev. Genet.* **2011**, *12*, 833–845. [CrossRef]
15. Rodriguez Barreto, D.; Rey, O.; Uren-Webster, T.M.; Castaldo, G.; Consuegra, S.; Garcia de Leaniz, C. Transcriptomic Response to Aquaculture Intensification in Nile Tilapia. *Evol. Appl.* **2019**, *12*, 1757–1771. [CrossRef]
16. Sun, P.; Bao, P.B.; Tang, B.J. Transcriptome Analysis and Discovery of Genes Involved in Immune Pathways in Large Yellow Croaker (*Larimichthys crocea*) under High Stocking Density Stress. *Fish Shellfish. Immunol.* **2017**, *68*, 332–340. [CrossRef]
17. He, Y.; Yu, H.Y.; Zhao, H.G.; Zhu, H.; Zhang, Q.J.; Wang, A.Q.; Shen, Y.B.; Xu, X.Y.; Li, J.L. Transcriptomic Analysis to Elucidate the Effects of High Stocking Density on Grass Carp (*Ctenopharyngodon idella*). *BMC Genom.* **2021**, *22*, 620. [CrossRef] [PubMed]
18. Liu, S.X.; Gao, G.T.; Palti, Y.; Cleveland, B.M.; Weber, G.M.; Iii, C.E.R. RNA-Seq Analysis of Early Hepatic Response to Handling and Confinement Stress in Rainbow Trout. *PLoS ONE* **2014**, *9*, e88492. [CrossRef] [PubMed]
19. Sánchez Muros, M.J.; Sánchez, B.; Barroso, F.G.; Toniolo, M.; Trenzado, C.E.; Sanz Rus, A. Effects of Rearing Conditions on Behavioural Responses, Social Kinetics and Physiological Parameters in Gilthead Sea Bream *Sparus aurata*. *Appl. Anim. Behav. Sci.* **2017**, *197*, 120–128. [CrossRef]
20. Fanouraki, E.; Divanach, P.; Pavlidis, M. Baseline Values for Acute and Chronic Stress Indicators in Sexually Immature Red Porgy (*Pagrus pagrus*). *Aquaculture* **2007**, *265*, 294–304. [CrossRef]
21. Chen, S.F.; Zhou, Y.Q.; Chen, Y.R.; Gu, J. Fastp: An Ultra-Fast All-in-One FASTQ Preprocessor. *Bioinformatics* **2018**, *34*, i884–i890. [CrossRef]
22. Langmead, B.; Salzberg, S.L. Fast Gapped-Read Alignment with Bowtie 2. *Nat. Methods* **2012**, *9*, 357–359. [CrossRef]
23. Kim, D.; Langmead, B.; Salzberg, S.L. HISAT: A Fast Spliced Aligner with Low Memory Requirements. *Nat. Methods* **2015**, *12*, 357–360. [CrossRef]
24. Pertea, M.; Pertea, G.M.; Antonescu, C.M.; Chang, T.-C.; Mendell, J.T.; Salzberg, S.L. StringTie Enables Improved Reconstruction of a Transcriptome from RNA-Seq Reads. *Nat. Biotechnol.* **2015**, *33*, 290–295. [CrossRef] [PubMed]
25. Li, B.; Dewey, C.N. RSEM: Accurate Transcript Quantification from RNA-Seq Data with or without a Reference Genome. *BMC Bioinform.* **2011**, *12*, 323. [CrossRef] [PubMed]
26. Love, M.I.; Huber, W.; Anders, S. Moderated Estimation of Fold Change and Dispersion for RNA-Seq Data with DESeq2. *Genome Biol.* **2014**, *15*, 550. [CrossRef]
27. Gene Ontology Consortium; Aleksander, S.A.; Balhoff, J.; Carbon, S.; Cherry, J.M.; Drabkin, H.J.; Ebert, D.; Feuermann, M.; Gaudet, P.; Harris, N.L.; et al. The Gene Ontology Knowledgebase in 2023. *Genetics* **2023**, *224*, iyad031. [CrossRef] [PubMed]
28. Ashburner, M.; Ball, C.A.; Blake, J.A.; Botstein, D.; Butler, H.; Cherry, J.M.; Davis, A.P.; Dolinski, K.; Dwight, S.S.; Eppig, J.T.; et al. Gene Ontology: Tool for the Unification of Biology. The Gene Ontology Consortium. *Nat. Genet.* **2000**, *25*, 25–29. [CrossRef]
29. Kanehisa, M.; Goto, S. KEGG: Kyoto Encyclopedia of Genes and Genomes. *Nucleic Acids Res.* **2000**, *28*, 27–30. [CrossRef] [PubMed]
30. Livak, K.J.; Schmittgen, T.D. Analysis of Relative Gene Expression Data Using Real-Time Quantitative PCR and the $2^{-\Delta\Delta CT}$ Method. *Meth. Mol. Biol.* **2001**, *25*, 402–408. [CrossRef]
31. Wei, M.L.; Shen, M.J.; Wang, Y.; Gao, B.; Sun, R.J.; Qin, Y.L.; Jiang, J.B.; Zhou, J.L.; Shen, J.; Tang, X.J.; et al. A Cold-Inducible RNA Binding Protein Gene from *Acanthopagrus schlegelii*: Molecular Characterization, Expression, and Association with Apoptosis to Low-Temperature Stress. *Aquac. Res.* **2023**, *2023*, e1697400. [CrossRef]
32. Li, X.J.; Shen, Y.D.; Bao, Y.G.; Wu, Z.X.; Yang, B.Q.; Jiao, L.F.; Zhang, C.D.; Tocher, D.R.; Zhou, Q.C.; Jin, M. Physiological Responses and Adaptive Strategies to Acute Low-Salinity Environmental Stress of the Euryhaline Marine Fish Black Seabream (*Acanthopagrus schlegelii*). *Aquaculture* **2022**, *554*, 738117. [CrossRef]
33. Shi, Q.C.; Yu, C.Q.; Zhu, D.S.; Li, S.K.; Wen, X.B. Effects of Dietary Sargassum Horneri on Resisting Hypoxia Stress, Which Changes Blood Biochemistry, Antioxidant Status, and Hepatic HSP mRNA Expressions of Juvenile Black Sea Bream *Acanthopagrus schlegelii*. *J. Appl. Phycol.* **2020**, *32*, 3457–3466. [CrossRef]
34. Tegomo, F.A.; Zhong, Z.W.; Njomoue, A.P.; Okon, S.U.; Ullah, S.; Gray, N.A.; Chen, K.; Sun, Y.X.; Xiao, J.X.; Wang, L.; et al. Experimental Studies on the Impact of the Projected Ocean Acidification on Fish Survival, Health, Growth, and Meat Quality; Black Sea Bream (*Acanthopagrus schlegelii*), Physiological and Histological Studies. *Animals* **2021**, *11*, 3119. [CrossRef]
35. Qiu, Y.Y.; Zhang, Z.Y.; Chen, S.Y.; Ni, K.W.; Jia, C.F.; Meng, Q.; Zhu, F.; Zhang, Z.W.; Tang, X.J. Comparative Study on feeding frequency of hybrid F_2 of *Acanthopagrus schlegelii* ♀× *Pagrus major*♂and *A. schlegelii*. *South China Fish. Sci.* **2022**, *18*, 59–67. [CrossRef]
36. Portz, D.E.; Woodley, C.M.; Cech, J.J. Stress-Associated Impacts of Short-Term Holding on Fishes. *Rev. Fish Biol. Fish.* **2006**, *16*, 125–170. [CrossRef]
37. Qi, L.J.; Chen, Y.D.; Shi, K.P.; Ma, H.; Wei, S.; Sha, Z.X. Combining of Transcriptomic and Proteomic Data to Mine Immune-Related Genes and Proteins in the Liver of *Cynoglossus semilaevis* Challenged with *Vibrio anguillarum*. *Comp. Biochem. Physiol. Part D Genom. Proteom.* **2021**, *39*, 100864. [CrossRef] [PubMed]
38. Wang, M.Y.; Xu, G.C.; Tang, Y.K.; Su, S.Y.; Wang, Y.P.; Zhu, Z.X. Investigation of the Molecular Mechanisms of Antioxidant Damage and Immune Response Downregulation in Liver of *Coilia nasus* under Starvation Stress. *Front. Endocrinol.* **2021**, *12*, 622315. [CrossRef] [PubMed]

39. Ghafoory, S.; Breitkopf-Heinlein, K.; Li, Q.; Scholl, C.; Dooley, S.; Wölfl, S. Zonation of Nitrogen and Glucose Metabolism Gene Expression upon Acute Liver Damage in Mouse. *PLoS ONE* **2013**, *8*, e78262. [CrossRef] [PubMed]
40. Liu, S.K.; Wang, X.L.; Sun, F.Y.; Zhang, J.R.; Feng, J.B.; Liu, H.; Rajendran, K.V.; Sun, L.Y.; Zhang, Y.; Jiang, Y.L.; et al. RNA-Seq Reveals Expression Signatures of Genes Involved in Oxygen Transport, Protein Synthesis, Folding, and Degradation in Response to Heat Stress in Catfish. *Physiol. Genom.* **2013**, *45*, 462–476. [CrossRef]
41. Tian, C.X.; Lin, X.H.; Saetan, W.; Huang, Y.; Shi, H.J.; Jiang, D.N.; Chen, H.P.; Deng, S.P.; Wu, T.L.; Zhang, Y.L.; et al. Transcriptome Analysis of Liver Provides Insight into Metabolic and Translation Changes under Hypoxia and Reoxygenation Stress in Silver Sillago (*Sillago sihama*). *Comp. Biochem. Physiol. Part D Genom. Proteom.* **2020**, *36*, 100715. [CrossRef]
42. Evans, T.G.; Kültz, D. The Cellular Stress Response in Fish Exposed to Salinity Fluctuations. *J. Exp. Zool. Part A Ecol. Integr. Physiol.* **2020**, *333*, 421–435. [CrossRef]
43. Naderi, M.; Keyvanshokooh, S.; Ghaedi, A.; Salati, A.P. Effect of Acute Crowding Stress on Rainbow Trout (*Oncorhynchus mykiss*): A Proteomics Study. *Aquaculture* **2018**, *495*, 106–114. [CrossRef]
44. McClain, W.H. Rules That Govern tRNA Identity in Protein Synthesis. *J. Mol. Biol.* **1993**, *234*, 257–280. [CrossRef]
45. Fromont Racine, M.; Senger, B.; Saveanu, C.; Fasiolo, F. Ribosome Assembly in Eukaryotes. *Gene* **2003**, *313*, 17–42. [CrossRef] [PubMed]
46. Zhu, J.L.; Zou, Z.Y.; Li, D.Y.; Xiao, W.; Yu, J.; Chen, B.L.; Xue, L.Y.; Yang, H. Transcriptome Profiling Revealed Basis for Growth Heterosis in Hybrid Tilapia (*Oreochromis niloticus* ♀× *O. aureus* ♂). *Fishes* **2022**, *7*, 43. [CrossRef]
47. Roh, H.; Kim, A.; Kim, N.; Lee, Y.; Kim, D.H. Multi-Omics Analysis Provides Novel Insight into Immuno-Physiological Pathways and Development of Thermal Resistance in Rainbow Trout Exposed to Acute Thermal Resistance. *Int. J. Mol. Sci.* **2020**, *21*, 9198. [CrossRef]
48. Chen, Y.J.; Wu, H.; Shen, X.Z. The Ubiquitin–Proteasome System and Its Potential Application in Hepatocellular Carcinoma Therapy. *Cancer Lett.* **2016**, *379*, 245–252. [CrossRef]
49. Peng, J.; Li, W.B.; Wang, B.; Zhang, S.; Xiao, Y.; Han, F.; Wang, Z.Y. UBE2G1 Is a Critical Component of Immune Response to the Infection of *Pseudomonas plecoglossicida* in Large Yellow Croaker (*Larimichthys crocea*). *Int. J. Mol. Sci.* **2022**, *23*, 8298. [CrossRef]
50. Groettrup, M.; Pelzer, C.; Schmidtke, G.; Hofmann, K. Activating the Ubiquitin Family: UBA6 Challenges the Field. *Trends Biochem. Sci.* **2008**, *33*, 230–237. [CrossRef] [PubMed]
51. Sun, J.L.; Zhao, L.L.; Wu, H.; Liu, Q.; Liao, L.; Luo, J.; Lian, W.Q.; Cui, C.; Jin, L.; Ma, J.D.; et al. Acute Hypoxia Changes the Mode of Glucose and Lipid Utilization in the Liver of the Largemouth Bass (*Micropterus salmoides*). *Sci. Total Environ.* **2020**, *713*, 135157. [CrossRef]
52. López Patiño, M.A.; Hernández Pérez, J.; Gesto, M.; Librán Pérez, M.; Míguez, J.M.; Soengas, J.L. Short-Term Time Course of Liver Metabolic Response to Acute Handling Stress in Rainbow Trout, *Oncorhynchus mykiss*. *Comp. Biochem. Physiol. Part A Mol. Integr. Physiol.* **2014**, *168*, 40–49. [CrossRef]
53. Wang, Y.L.; Meng, R.; Xu, X.R.; Liao, K.; Ran, Z.S.; Xu, J.L.; Cao, J.Y.; Wang, Y.J.; Wang, D.L.; Xu, S.L.; et al. Effects of Nutritional Status and Diet Composition on Fatty Acid Transporters Expression in Zebrafish (*Danio rerio*). *Aquac. Res.* **2019**, *50*, 904–914. [CrossRef]
54. Bayır, M.; Bayır, A.; Wright, J.M. Divergent Spatial Regulation of Duplicated Fatty Acid-Binding Protein (Fabp) Genes in Rainbow Trout (*Oncorhynchus mykiss*). *Comp. Biochem. Physiol. Part D Genom. Proteom.* **2015**, *14*, 26–32. [CrossRef] [PubMed]
55. Cheema, S.K.; Agellon, L.B. The Murine and Human Cholesterol 7alpha-Hydroxylase Gene Promoters Are Differentially Responsive to Regulation by Fatty Acids Mediated via Peroxisome Proliferator-Activated Receptor Alpha. *J. Biol. Chem.* **2000**, *275*, 12530–12536. [CrossRef] [PubMed]
56. Ameer, F.; Munir, R.; Zaidi, N. Lipid Metabolism. In *Encyclopedia of Cancer*, 3rd ed.; Boffetta, P., Hainaut, P., Eds.; Academic Press: Oxford, UK, 2019; pp. 369–373, ISBN 978-0-12-812485-7.
57. Lu, X.Y.; Shi, X.J.; Hu, A.; Wang, J.Q.; Ding, Y.; Jiang, W.; Sun, M.; Zhao, X.L.; Luo, J.; Qi, W.; et al. Feeding Induces Cholesterol Biosynthesis via the mTORC1–USP20–HMGCR Axis. *Nature* **2020**, *588*, 479–484. [CrossRef] [PubMed]
58. Glencross, B.D.; Santis, C.D.; Bicskei, B.; Taggart, J.B.; Bron, J.E.; Betancor, M.B.; Tocher, D.R. A Comparative Analysis of the Response of the Hepatic Transcriptome to Dietary Docosahexaenoic Acid in Atlantic Salmon (*Salmo salar*) Post-Smolts. *BMC Genom.* **2015**, *16*, 684. [CrossRef] [PubMed]
59. Gill, S.; Stevenson, J.; Kristiana, I.; Brown, A.J. Cholesterol-Dependent Degradation of Squalene Monooxygenase, a Control Point in Cholesterol Synthesis beyond HMG-CoA Reductase. *Cell Metab.* **2011**, *13*, 260–273. [CrossRef] [PubMed]
60. Sun, H.S.; Li, L.; Li, W.; Yang, F.; Zhang, Z.X.; Liu, Z.Z.; Du, W.J. P53 Transcriptionally Regulates SQLE to Repress Cholesterol Synthesis and Tumor Growth. *EMBO Rep.* **2021**, *22*, e52537. [CrossRef]
61. Gatticchi, L.; de las Heras, J.I.; Sivakumar, A.; Zuleger, N.; Roberti, R.; Schirmer, E.C. *Tm7sf2* Disruption Alters Radial Gene Positioning in Mouse Liver Leading to Metabolic Defects and Diabetes Characteristics. *Front. Cell Dev. Biol.* **2020**, *8*, 592573. [CrossRef]
62. Lewinska, M.; Juvan, P.; Perse, M.; Jeruc, J.; Kos, S.; Lorbek, G.; Urlep, Z.; Keber, R.; Horvat, S.; Rozman, D. Hidden Disease Susceptibility and Sexual Dimorphism in the Heterozygous Knockout of Cyp51 from Cholesterol Synthesis. *PLoS ONE* **2014**, *9*, e112787. [CrossRef]
63. Hui, D.Y.; Howles, P.N. Carboxyl Ester Lipase. *J. Lipid Res.* **2002**, *43*, 2017–2030. [CrossRef]

64. Jiang, T.; Liang, Y.S.; Gu, Y.; Yao, F.C.; Liu, Y.F.; Zhang, K.X.; Song, F.B.; Sun, J.L.; Luo, J. Different Reoxygenation Rates Induce Different Metabolic, Apoptotic and Immune Responses in Golden Pompano (*Trachinotus blochii*) after Hypoxic Stress. *Fish Shellfish. Immunol.* **2023**, *135*, 108640. [CrossRef]
65. Zhao, T.T.; Ma, A.J.; Huang, Z.H.; Liu, Z.F.; Sun, Z.B.; Zhu, C.Y.; Yang, J.K.; Li, Y.D.; Wang, Q.M.; Qiao, X.W.; et al. Transcriptome Analysis Reveals That High Temperatures Alter Modes of Lipid Metabolism in Juvenile Turbot (*Scophthalmus maximus*) Liver. *Comp. Biochem. Physiol. Part D Genom. Proteom.* **2021**, *40*, 100887. [CrossRef] [PubMed]
66. Gornati, R.; Papis, E.; Rimoldi, S.; Chini, V.; Terova, G.; Prati, M.; Saroglia, M.; Bernardini, G. Molecular Markers for Animal Biotechnology: Sea Bass (*Dicentrarchus labrax*, L.) HMG-CoA Reductase mRNA. *Gene* **2005**, *344*, 299–305. [CrossRef] [PubMed]
67. Montero, D.; Izquierdo, M.; Tort, L.; Robaina, L.; Vergara, J.M. High Stocking Density Produces Crowding Stress Altering Some Physiological and Biochemical Parameters in Gilthead Seabream, *Sparus aurata*, Juveniles. *Fish Physiol. Biochem.* **1999**, *20*, 53–60. [CrossRef]
68. Jia, R.; Wang, L.; Hou, Y.R.; Feng, W.R.; Li, B.; Zhu, J. Effects of Stocking Density on the Growth Performance, Physiological Parameters, Redox Status and Lipid Metabolism of *Micropterus salmoides* in Integrated Rice–Fish Farming Systems. *Antioxidants* **2022**, *11*, 1215. [CrossRef]
69. Raposo de Magalhães, C.; Schrama, D.; Nakharuthai, C.; Boonanuntanasarn, S.; Revets, D.; Planchon, S.; Kuehn, A.; Cerqueira, M.; Carrilho, R.; Farinha, A.P.; et al. Metabolic Plasticity of Gilthead Seabream under Different Stressors: Analysis of the Stress Responsive Hepatic Proteome and Gene Expression. *Front. Mar. Sci.* **2021**, *8*, 676189. [CrossRef]
70. Sivanand, S.; Rhoades, S.; Jiang, Q.Q.; Lee, J.V.; Benci, J.; Zhang, J.W.; Yuan, S.; Viney, I.; Zhao, S.; Carrer, A.; et al. Nuclear Acetyl-CoA Production by ACLY Promotes Homologous Recombination. *Mol. Cell* **2017**, *67*, 252–265. [CrossRef]
71. Corominas-Faja, B.; Cuyàs, E.; Gumuzio, J.; Bosch-Barrera, J.; Leis, O.; Martin, Á.G.; Menendez, J.A. Chemical Inhibition of Acetyl-CoA Carboxylase Suppresses Self-Renewal Growth of Cancer Stem Cells. *Oncotarget* **2014**, *5*, 8306–8316. [CrossRef]
72. Cronan, J.E.; Waldrop, G.L. Multi-Subunit Acetyl-CoA Carboxylases. *Prog. Lipid Res.* **2002**, *41*, 407–435. [CrossRef]
73. Bláhová, Z.; Harvey, T.N.; Pšenička, M.; Mráz, J. Assessment of Fatty Acid Desaturase (Fads2) Structure-Function Properties in Fish in the Context of Environmental Adaptations and as a Target for Genetic Engineering. *Biomolecules* **2020**, *10*, 206. [CrossRef]
74. de Lima Luna, A.C.; Forti, F.L. Modulation of SCD1 Activity in Hepatocyte Cell Lines: Evaluation of Genomic Stability and Proliferation. *Mol. Cell. Biochem.* **2021**, *476*, 3393–3405. [CrossRef]
75. Lehner, R.; Quiroga, A.D. Fatty Acid Handling in Mammalian Cells. In *Biochemistry of Lipids, Lipoproteins and Membranes*, 7th ed.; Ridgway, N.D., McLeod, R.S., Eds.; Elsevier: Amsterdam, The Netherlands, 2021; pp. 161–200. ISBN 978-0-12-824048-9.
76. Berthelot, K.; Estevez, Y.; Deffieux, A.; Peruch, F. Isopentenyl Diphosphate Isomerase: A Checkpoint to Isoprenoid Biosynthesis. *Biochimie* **2012**, *94*, 1621–1634. [CrossRef]
77. Neufeld, E.B.; Demosky, S.J.; Stonik, J.A.; Combs, C.; Remaley, A.T.; Duverger, N.; Santamarina-Fojo, S.; Brewer, H.B. The ABCA1 Transporter Functions on the Basolateral Surface of Hepatocytes. *Biochem. Biophys. Res. Commun.* **2002**, *297*, 974–979. [CrossRef]
78. Pickering, A.D.; Pottinger, T.G. Stress Responses and Disease Resistance in Salmonid Fish: Effects of Chronic Elevation of Plasma Cortisol. *Fish Physiol. Biochem.* **1989**, *7*, 253–258. [CrossRef] [PubMed]
79. Hoseini, S.M.; Abtahi, B.; Yousefi, M. Effects of Fasting on Metabolic and Immunological Responses of Common Carp (*Cyprinus carpio*) to a Further Acute Stress. *Aquac. Res.* **2019**, *50*, 1177–1185. [CrossRef]
80. Varga, T.; Czimmerer, Z.; Nagy, L. PPARs Are a Unique Set of Fatty Acid Regulated Transcription Factors Controlling Both Lipid Metabolism and Inflammation. *Biochim. Et Biophys. Acta (BBA) Mol. Basis Dis.* **2011**, *1812*, 1007–1022. [CrossRef] [PubMed]
81. Wang, Y.P.; Nakajima, T.; Gonzalez, F.J.; Tanaka, N. PPARs as Metabolic Regulators in the Liver: Lessons from Liver-Specific PPAR-Null Mice. *Int. J. Mol. Sci.* **2020**, *21*, 2061. [CrossRef]
82. Liu, W.; Wang, X.; Liu, Y.; Fang, S.Y.; Wu, Z.J.; Han, C.; Shi, W.Y.; Bao, Y.Z. Effects of Early Florfenicol Exposure on Glutathione Signaling Pathway and PPAR Signaling Pathway in Chick Liver. *Ecotoxicol. Environ. Saf.* **2022**, *237*, 113529. [CrossRef]
83. Xu, H.G.; Zhang, X.; Wei, Y.L.; Sun, B.; Jia, L.L.; Liang, M.Q. Effects of Dietary Phosphorus Level and Stocking Density on Tiger Puffer *Takifugu rubripes*: Growth Performance, Body Composition, Lipid Metabolism, Deposition of Phosphorus and Calcium, Serum Biochemical Parameters, and Phosphorus Excretion. *Aquaculture* **2020**, *529*, 735709. [CrossRef]
84. Cao, X.F.; Liu, W.B.; Ai, Q.H.; Li, X.S.; Li, J.B.; Fang, W.; Huang, Y.Y.; Wang, C.C.; Jiang, G.Z. High-fat Diet-induced Inflammation Aggravates Hepatic Steatosis of Blunt Snout Bream (*Megalobrama amblycephala*) through the Transcription Regulation of Fatty Acid Synthesis and Oxidation. *Aquacult. Nutr.* **2020**, *26*, 1493–1504. [CrossRef]
85. Xu, C.; Li, E.; Liu, S.; Huang, Z.P.; Qin, J.G.; Chen, L.Q. Effects of α-Lipoic Acid on Growth Performance, Body Composition, Antioxidant Status and Lipid Catabolism of Juvenile Chinese Mitten Crab *Eriocheir sinensis* Fed Different Lipid Percentage. *Aquaculture* **2018**, *484*, 286–292. [CrossRef]
86. Anders, N.; Roth, B.; Breen, M. Physiological Response and Survival of Atlantic Mackerel Exposed to Simulated Purse Seine Crowding and Release. *Conserv. Physiol.* **2021**, *9*, coab076. [CrossRef]
87. Dhabhar, F.S. The Power of Positive Stress—A Complementary Commentary. *Stress* **2019**, *22*, 526–529. [CrossRef] [PubMed]
88. Guo, H.; Dixon, B. Understanding Acute Stress-Mediated Immunity in Teleost Fish. *Fish Shellfish. Immunol. Rep.* **2021**, *2*, 100010. [CrossRef] [PubMed]
89. Zhao, L.L.; Sun, J.L.; Liang, J.; Liu, Q.; Luo, J.; Li, Z.Q.; Yan, T.M.; Zhou, J.; Yang, S. Enhancing Lipid Metabolism and Inducing Antioxidant and Immune Responses to Adapt to Acute Hypoxic Stress in *Schizothorax prenanti*. *Aquaculture* **2020**, *519*, 734933. [CrossRef]

90. Okoye, C.N.; Chinnappareddy, N.; Stevens, D.; Kamunde, C. Factors Affecting Liver Mitochondrial Hydrogen Peroxide Emission. *Comp. Biochem. Physiol. Part B Biochem. Mol. Biol.* **2022**, *259*, 110713. [CrossRef] [PubMed]
91. Cannito, S.; Novo, E.; Parola, M. Therapeutic Pro-Fibrogenic Signaling Pathways in Fibroblasts. *Adv. Drug Deliv. Rev.* **2017**, *121*, 57–84. [CrossRef]
92. Liu, J.; Zhu, K.C.; Pan, J.M.; Guo, H.Y.; Liu, B.S.; Zhang, N.; Yang, J.W.; Zhang, D.C. Characterization of the *MMP9* Gene and Its Association with *Cryptocaryon irritans* Resistance Traits in *Trachinotus ovatus* (Linnaeus, 1758). *Genes* **2023**, *14*, 475. [CrossRef]
93. Kluger, M.A.; Zahner, G.; Paust, H.-J.; Schaper, M.; Magnus, T.; Panzer, U.; Stahl, R.A.K. Leukocyte-Derived MMP9 Is Crucial for the Recruitment of Proinflammatory Macrophages in Experimental Glomerulonephritis. *Kidney Int.* **2013**, *83*, 865–877. [CrossRef] [PubMed]
94. Zheng, X.P.; Deng, F.; Sharma, I.; Kanwar, Y.S. Myo-Inositol Oxygenase Overexpression Exacerbates Cadmium-Induced Kidney Injury via Oxidant Stress and Necroptosis. *Am. J. Physiol. Ren. Physiol.* **2022**, *322*, F344–F359. [CrossRef]
95. Yoshihara, D.; Fujiwara, N.; Ookawara, T.; Kato, S.; Sakiyama, H.; Yokoe, S.; Eguchi, H.; Suzuki, K. Protective Role of Glutathione S-Transferase A4 Induced in Copper/Zinc-Superoxide Dismutase Knockout Mice. *Free. Radic. Biol. Med.* **2009**, *47*, 559–567. [CrossRef]
96. Ramming, T.; Hansen, H.G.; Nagata, K.; Ellgaard, L.; Appenzeller-Herzog, C. GPx8 Peroxidase Prevents Leakage of H_2O_2 from the Endoplasmic Reticulum. *Free. Radic. Biol. Med.* **2014**, *70*, 106–116. [CrossRef]
97. Berry, F.B.; Skarie, J.M.; Mirzayans, F.; Fortin, Y.; Hudson, T.J.; Raymond, V.; Link, B.A.; Walter, M.A. FOXC1 Is Required for Cell Viability and Resistance to Oxidative Stress in the Eye through the Transcriptional Regulation of FOXO1A. *Hum. Mol. Genet.* **2008**, *17*, 490–505. [CrossRef]
98. Ortuño, J.; Esteban, M.A.; Meseguer, J. Effects of Short-Term Crowding Stress on the Gilthead Seabream (*Sparus aurata* L.) Innate Immune Response. *Fish Shellfish. Immunol.* **2001**, *11*, 187–197. [CrossRef]
99. Huang, X.J.; Xu, Y.L.; Yang, Q.Y.; Chen, J.Q.; Zhang, T.; Li, Z.C.; Guo, C.P.; Chen, H.; Wu, H.; Li, N. Efficacy and Biological Safety of Lopinavir/Ritonavir Based Anti-Retroviral Therapy in HIV-1-Infected Patients: A Meta-Analysis of Randomized Controlled Trials. *Sci. Rep.* **2015**, *5*, 8528. [CrossRef] [PubMed]
100. Xiong, M.; Kommaly, O.; Li, D.P.; Wang, H.S.; Liang, X.; Tang, R.; Li, L.; Zhang, X.; Chi, W. Effect of acute crowding stress on the ubiquitin-proteasome system in the muscle of grass carp (*Ctenopharyngodon idellus*). *J. Fish. Sci. China* **2019**, *26*, 427. [CrossRef]
101. Yada, T.; Tort, L. Stress and Disease Resistance: Immune System and Immunoendocrine Interactions. In *Fish Physiology*; Schreck, C.B., Tort, L., Farrell, A.P., Brauner, C.J., Eds.; Biology of Stress in Fish; Academic Press: Cambridge, MA, USA, 2016; Volume 35, pp. 365–403.
102. Huo, H.H.; Gao, X.Q.; Fei, F.; Qin, F.; Huang, B.; Liu, B.L. Transcriptomic Profiling of the Immune Response to Crowding Stress in Juvenile Turbot (*Scophthalmus maximus*). *J. Ocean. Univ. China* **2020**, *19*, 911–922. [CrossRef]
103. Jia, R.; Liu, B.L.; Feng, W.R.; Han, C.; Huang, B.; Lei, J.L. Stress and Immune Responses in Skin of Turbot (*Scophthalmus maximus*) under Different Stocking Densities. *Fish Shellfish. Immunol.* **2016**, *55*, 131–139. [CrossRef]
104. Ellison, A.R.; Uren Webster, T.M.; Rodriguez-Barreto, D.; de Leaniz, C.G.; Consuegra, S.; Orozco ter Wengel, P.; Cable, J. Comparative Transcriptomics Reveal Conserved Impacts of Rearing Density on Immune Response of Two Important Aquaculture Species. *Fish Shellfish. Immunol.* **2020**, *104*, 192–201. [CrossRef] [PubMed]
105. Yarahmadi, P.; Miandare, H.K.; Fayaz, S.; Caipang, C.M.A. Increased Stocking Density Causes Changes in Expression of Selected Stress- and Immune-Related Genes, Humoral Innate Immune Parameters and Stress Responses of Rainbow Trout (*Oncorhynchus mykiss*). *Fish Shellfish. Immunol.* **2016**, *48*, 43–53. [CrossRef]
106. Haase, D.; Rieger, J.K.; Witten, A.; Stoll, M.; Bornberg-Bauer, E.; Kalbe, M.; Schmidt-Drewello, A.; Scharsack, J.P.; Reusch, T.B.H. Comparative Transcriptomics of Stickleback Immune Gene Responses upon Infection by Two Helminth Parasites, *Diplostomum pseudospathaceum* and *Schistocephalus solidus*. *Zoology* **2016**, *119*, 307–313. [CrossRef]
107. Wang, T.; Liang, J.; Xiang, X.; Yuan, J.; Chen, X.; Xiang, X.; Yang, J. Functional Identification and Expressional Responses of Large Yellow Croaker (*Larimichthys crocea*) Interleukin-8 and Its Receptor. *Fish Shellfish. Immunol.* **2019**, *87*, 470–477. [CrossRef] [PubMed]
108. Shariat, M.; Heydrzadeh, M.; Abolhassani, H.; Bemanian, M.; Yazdani, R. Complement Deficiencies. In *Inborn Errors of Immunity*; Academic Press: Cambridge, MA, USA, 2021; pp. 291–315. ISBN 978-0-12-821028-4.
109. Sarma, J.V.; Ward, P.A. The Complement System. *Cell Tissue Res.* **2011**, *343*, 227–235. [CrossRef] [PubMed]
110. Arlaud, G.J.; Gaboriaud, C.; Thielens, N.M.; Budayova-Spano, M.; Rossi, V.; Fontecilla Camps, J.C. Structural Biology of the C1 Complex of Complement Unveils the Mechanisms of Its Activation and Proteolytic Activity. *Mol. Immunol.* **2002**, *39*, 383–394. [CrossRef]
111. Lin, W.; Li, L.; Chen, J.; Li, D.P.; Hou, J.; Guo, H.H.; Shen, J.Z. Long-Term Crowding Stress Causes Compromised Nonspecific Immunity and Increases Apoptosis of Spleen in Grass Carp (*Ctenopharyngodon idella*). *Fish Shellfish. Immunol.* **2018**, *80*, 540–545. [CrossRef] [PubMed]